

AD619179

STABILITY OF HIGH STRENGTH H₂O₂QUARTERLY REPORT FOR PERIOD ENDING JUNE 30, 1965

ELECTROCHEMICALS DEPARTMENT
E. I. DU PONT DE NEMOURS & CO.
WILMINGTON, DEL.

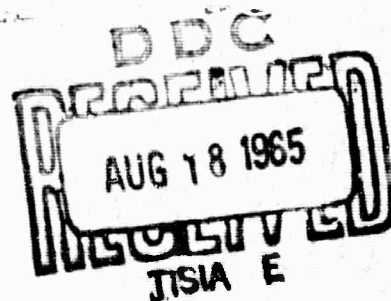
| | | |
|------------|----------|-----------|
| COPY _____ | OF _____ | 1 as |
| HARD COPY | | \$. 2.00 |
| MICROFICHE | | \$. 0.50 |

398

CONTRACT NO. AF 04(611)-10216

SPONSORED BY

ADVANCED RESEARCH PROJECTS AGENCY
WASHINGTON 25, D.C.
ARPA ORDER NO. 24



NEGATIVE COPY

INTRODUCTION

This is the third quarterly report on this program. The experimental work is being carried out in two locations: the Niagara Falls Research Laboratories of the Electrochemicals Department, and the Radiation Physics Laboratory of the Engineering Department, of E. I. du Pont de Nemours & Co. The report is therefore divided into two sections, based on location of the work.

The objectives of this program are stated in the contract as follows:

1. The Contractor shall conduct a research program consisting of the following phases:

- a. Determine the inherent bulk stability of pure 90 to 100% hydrogen peroxide at temperatures ranging from -60°F. to $+160^{\circ}\text{F.}$ in the absence of catalyzing surfaces by using solid hydrogen peroxide as the wall.
- b. Determine the effect of wall surfaces on the bulk stability as secured above by electron spin resonance and infrared attenuated total reflectance techniques employed on the interface.
- c. To subject the pure hydrogen peroxide in contact with a stable surface, if one is found, to radiation to induce instability and thus generate radicals whose interactions with the surface can be determined. The choice and use of the stable surface, if found, will be mutually agreed upon by the procuring activity and the contractor before this phase of study commences.

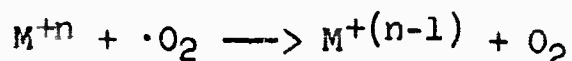
2. This program shall be directed toward the gathering of information affecting the storability of hydrogen peroxide. Emphasis will lie on the reliability and reproducibility of the data attained.

SUMMARY

1. At Niagara Falls, studies of low temperature (-60°C. to 0°C.) storage of 90% and 98% hydrogen peroxide, both commercial (stabilized) and high purity (unstabilized) in passivated Pyrex glass have been completed. Conclusions are the same as earlier reported: (1) At -60°C. (solid state) no decomposition of 90% or 98% hydrogen peroxide can be detected; (2) at -30°C. , with 98% hydrogen peroxide (solid state) no decomposition can be detected, with 90% material (trace of liquid) decomposition is barely detectable; (3) at 0°C. , with all samples liquid, decomposition rates vary, depending on the source of the hydrogen peroxide, from undetectable to a maximum of 5 ppm/day (less than 0.2% per year).

2. Work during this quarter at the Radiation Physics Laboratory has been devoted to improving the electron paramagnetic resonance equipment especially by the addition of a fast closing valve (100 μ sec.), thus damping out oscillations caused by stopping the flow, and allowing observation of events in the reaction of neutral solutions of $TiCl_3$ and H_2O_2 in the 1-100 m sec. time range. Using this modified equipment, the maximum radical signal for a steady state flow was observed about 50 m sec. after the opening of the valve. This signal increased about one-third in 50 m sec. on closing the valve, and then decayed to one-half its value in about 200 m sec. This system is now an excellent tool to follow the radical growth and decay in peroxide reactions.

3. To enable direct calculations of rate constants for these reactions, optical absorption studies on the products of the reaction have been begun. The unit as now assembled allows recording of transient intermediates (radicals) along 0.5 mm. portions of the 5 cm. long flow stream. The first results from this optical system have resulted in demonstration of a superoxide radical ($\cdot O_2$) "generator", which will allow rate constants to be determined on the reduction step involving this radical:



4. Studies on inert surfaces for possible container use for high strength hydrogen peroxide have shown that irradiated "Teflon" FEP fluorocarbon resin containers allow storage of such hydrogen peroxide with between one-half and one-third the decomposition encountered in carefully passivated aluminum or Pyrex glass. This observation is being further explored.

Detailed discussion of the experimental work follows.

Section A - Work at the Niagara Falls Research Laboratories - A.M. Stock

I. Rate of Decomposition of High Strength H_2O_2

Decomposition rates at $-30^\circ C.$ and $0^\circ C.$ have been determined for the second series of H_2O_2 samples. (This series included both commercial and specially purified unstabilized H_2O_2 ; a detailed description of the samples can be found in the preceding quarterly report¹). At $-30^\circ C.$, the observed decomposition rates (Table S-1, Figure S-1) were below the level of statistical significance or of marginal statistical significance at most. The "negative" rates reported (Table S-1) for samples 9 through 12 can be attributed to failure of the samples to reach thermal equilibrium at the time of the initial observation. The rate

plots in Figure S-1 show either little change or a slight increasing trend in the amount of H_2O_2 decomposed after the second observation. At $0^\circ C.$, five of the samples (#1, 2, 6, 10, and 11) decomposed at statistically significant rates. The calculated decomposition rates of samples #4, 5 and 12 were of marginal statistical significance; and those of the remaining samples were below the level of statistical significance. The low decomposition rates of the unstabilized samples indicate that a high degree of stability is possible without stabilizers, provided high purity is maintained. In this group of samples (#1 through #6) there seemed to be at least a rough correlation between higher conductance and higher decomposition rate. The behavior of the various commercial samples (#7 through #12) was about the same as it had been in the first series of experiments, with one exception - the decomposition rate of the 90% H_2O_2 from Manufacturer C was higher than expected from the previous results. The conductance measurements do not indicate ionic contamination of the sample, although contamination by a nonionic material such as silicone grease remains a possibility. In any case, the highest decomposition rates observed at $0^\circ C.$ (ca. 3.5 ppm/day) are in agreement with those found in the first series of experiments (3 to 5 ppm/day).

The conclusions of the two series of decomposition rate studies can be summarized as follows:

1. At $-60^\circ C.$ solid hydrogen peroxide showed no evidence of decomposition regardless of the presence or absence of stabilizers.
2. The onset of decomposition was associated with the appearance of a liquid phase at about $-30^\circ C.$ in the case of 90% H_2O_2 and at somewhat higher temperatures in the case of 98% H_2O_2 .
3. In the liquid phase ($0^\circ C.$), decomposition rates of commercial high strength (90% and 98%) H_2O_2 ranged from a maximum of about 5 ppm/day to below the level of statistical significance.
4. Carefully purified unstabilized H_2O_2 was only slightly less stable than the most stable commercial H_2O_2 and considerably more stable than the least stable commercial H_2O_2 , indicating that stabilizers are not required for high stability provided high purity is maintained.
5. There was only a rough correlation between low electrical conductivity and high stability, indicating that electrical conductivity per se is not a reliable indicator of stability.

Section B - Work at the Radiation Physics Laboratory,
Wilmington, Delaware

- J. P. Paris

I. Introduction

High-strength hydrogen peroxide in the absence of impurities and stabilizers is a very stable material, as indicated by Dr. Stock's data on high purity samples. However, most samples of

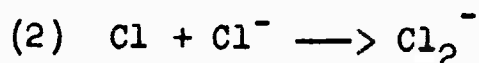
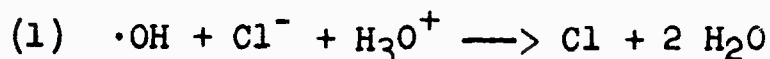
hydrogen peroxide in common use are slightly contaminated with metal ions accidentally added either in manufacture or on storage in aluminum containers. For this reason, our research has been directed towards (a) determining the reaction mechanism of the metal ion catalyzed decomposition and (b) finding inert container materials.

II. Reaction Mechanisms

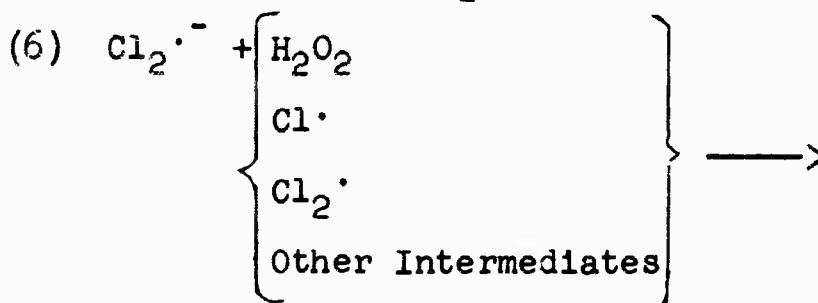
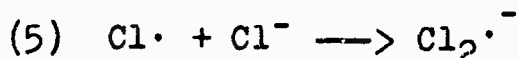
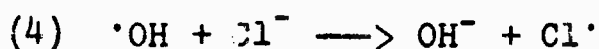
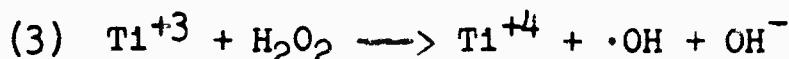
The free radicals formed in the decomposition of hydrogen peroxide include $\cdot\text{OH}$, $\cdot\text{O}^-$, $\cdot\text{O}_2\text{H}$ and $\cdot\text{O}_2^-$ depending on the pH of the system. The methods of generation and observation of these species were summarized in the last quarterly report. Because of the high reactivity of these intermediates, their concentrations in solutions are extremely low (10^{-4} - 10^{-7} M) and therefore require very sensitive detection methods. The two methods chosen for this study are (a) electron paramagnetic resonance (EPR) and (b) optical absorption spectroscopy.

A brief review of the reactions initiated by the hydroxyl radical is necessary to supplement that outlined in the last quarterly report. In addition to those 33 reactions involved in the metal cation-hydrogen peroxide system, there is a simultaneous series of competing reactions with the anions. Of particular importance are the reactions of chloride and hydrogen sulfate in the acid catalyzed decomposition of hydrogen peroxide by titanium trichloride.

The rate constants for the reaction of hydroxyl radicals with halogen ions are tabulated in Table I. Anbar and Thomas², using pulse radiolysis studies on aqueous sodium chloride solutions, identified the major transient in the reaction as Cl_2^- . The rate of formation of Cl_2^- was independent of oxygen concentration, first order in $[\text{H}^+]$ from pH 3 to 0, and first order in chloride ion and hydroxyl radical concentration. The pH dependence was suggested to result from the following reactions:

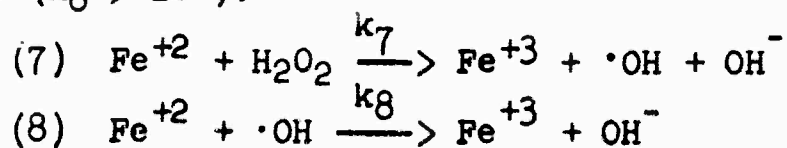


With respect to the titanium trichloride reduction of hydrogen peroxide in strongly acidic solutions, the following series of reactions may be the most important:



The prevalence of chlorine atom intermediates is further indicated by certain organic chlorination reactions. For example, using hydrogen peroxide modified with HCl, Marsh³ produced 2,4,6-trichlorophenol from phenol, Jurd⁴ produced 4-chloroanisole from anisole, and Johnson⁵ chlorinated 2,4-diketotetrahydropyrimidines.

Table II shows the rate constants for the oxidation of certain metal ions with hydroxyl radicals. The conclusion to be drawn from these data is that if the initiation of the reaction of hydrogen peroxide with the metal ion is slow ($k_7 < 10^3$), the transient hydroxyl radical cannot be easily observed by EPR or optical spectroscopy. This results from the competition reaction 8 ($k_8 > 10^8$):



Under the optimum conditions of high H_2O_2 concentrations ($> 1 \text{ M}$) and low Fe^{+2} concentrations ($< 10^{-3} \text{ M}$), no transient radicals have been observed.

Further complications due to anions are indicated by the data shown in Table III. Whereas sulfuric acid is normally assumed to contribute to the reaction scheme only by changing pH, one must also include the reaction of hydroxyl radicals with HSO_4^- ($k = 3.3 \times 10^7 \text{ M}^{-1} \text{ sec}^{-1}$).

III. Experimental Results on Reaction Mechanisms

The scope of the EPR studies was greatly extended by the incorporation of a fast closing (100 μsec) valve at the exit of the flow system previously described. The two reactants are mixed in the quartz mixing chamber in 1-2 msec, then directed through the EPR cavity in a flat quartz cell having the ballistic valve attached to the exit port. The advantage of having a very fast valve compared to the mixing and flow of the solution is that the oscillations caused by stopping the flow are damped out in a few hundred microseconds. Therefore, the events observed in the 1-100 msec time range are unaffected by the valve mechanism.

Figure 1 shows the growth and decay of the radical intermediate observed in the reaction of $1.3 \times 10^{-2} \text{ M}$ titanium trichloride with 1.3 M hydrogen peroxide. After mixing, the initial concentrations should be $6.5 \times 10^{-3} \text{ M Ti}^{+3}$, $1.9 \times 10^{-2} \text{ M Cl}^-$, and 0.65 M H_2O_2 . Elimination of the interfering reactions with the Cl^- and HSO_4^- ions was accomplished by working in neutral solutions (no H_2SO_4 added). Since the reaction of hydroxyl radicals with chloride ions is slow in neutral solutions ($< 10^7 \text{ M}^{-1} \text{ sec}^{-1}$) as contrasted to $4 \times 10^9 \text{ M}^{-1} \text{ sec}^{-1}$ at pH 0, the principal reaction of $\cdot\text{OH}$ should be with H_2O_2 ($k = 4.5 \times 10^7 \text{ M}^{-1} \text{ sec}^{-1}$) to give $\cdot\text{O}_2$ ($\text{pK HO}_2\cdot = 4.5$).

At this point A, in Figure 1, the flow was started by opening the valve. Solution of equal proportions of 1.3×10^{-2} M $TiCl_3$ and 1.3 M H_2O_2 were mixed at a combined flow rate of 300 cc/minute. The maximum signal for a steady flow of 300 cc/minute was observed at point B, approximately 50 msec after the valve was opened. Closing the valve (point C) caused a further increase in signal level to point D. The transient radical concentration then decayed to one-half of its maximum value in about 200 msec.

The stopped flow studies on neutral solutions using fast flow rates indicated that achieving the maximum free radical signal required a growth time of about 5 msec. This feature of the reaction was supported by data obtained on decreasing the flow rate from 300 cc/minute to 150 cc/minute. The slower flow rate increased the signal level 30% and eliminated the growth to a maximum after closing the valve.

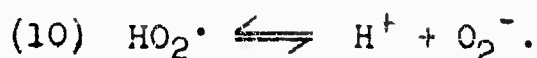
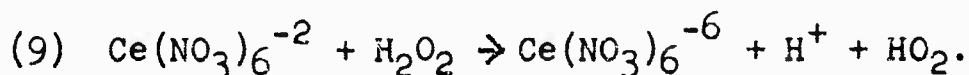
Direct calculations of rate constants for the $Ti^{+3} - H_2O_2$ reaction are not possible as yet because of the assumptions necessary for the initiating step. Optical absorption studies on the reactants and products of this reaction are in progress to provide these data. The flow cell combined with the Cary 14 absorption spectrophotometer is shown in Figure 2.

Use of the flow system for optical studies permits the recording of transient intermediates at various points down the sample cell. The quartz cell presents a 0.5 mm path length to the analyzing light beam and has an adjustable slit along the flow stream of 5 cm. Because of the short path length of the cell, a slide wire having a full scale deflection of 0.1 absorbance units was installed to increase the sensitivity of the measurements. Concentrations of 10^{-4} M of transients having $\epsilon > 10^3$ can easily be detected with this system.

To avoid some of the numerous side reactions induced by the hydroxyl radical, a study was initiated using the well-known ceric ion oxidation of hydrogen peroxide to produce perhydroxyl radicals.⁸ Working in strongly acidic solutions, Saito and Bielski^{7,8} reported an EPR single line spectrum with $g = 2.016$ and a line width of 27 gauss formed in a flow system of ceric sulfate and hydrogen peroxide. Using ceric ammonium nitrate and hydrogen peroxide in acid solution, Piette, Bulow and Loeffler⁹ observed a single line at $g = 2.0185$ having a line width of 1 gauss. Our studies confirmed these results and showed very erratic effects dependent on acid strength.

The chemistry of the ceric ion is dependent on its particular complex in solution. Ceric sulfate in dilute solutions of sulfuric acid forms the sulfato-cerate complex, $Ce(SO_4)_4^{-4}$, whereas ceric ammonium nitrate is originally in the nitrate-cerate form $Ce(NO_3)^{-2}$. The only form of Ce^{+4} never observed (contrary to the reactions normally written) is that indicated as the free ion. Since the reactions of the cerate ions with hydrogen peroxide involve electron transfer, one of the most important properties of the system is the effect of complexing on the electrode potential. Standard electrode potentials for ceric complexes vary from 1.28 to 1.70 volts depending on the acid present (HCl , 1.28 V; H_2SO_4 , 1.44 V; HNO_3 , 1.61 V; $HClO_4$, 1.70V).¹⁰

To avoid the complex equilibrium of anions in the ceric co-ordination sphere, the reaction of the nitrate-cerate ion with hydrogen peroxide was carried out in neutral solutions. A very strong single line spectrum having a line width of about 1 gauss was found which is assigned to the superoxide ion. The reaction sequence postulated is:



Absorption spectra were taken on the nitrate- and sulfato-ceric complexes for their analysis in the optical flow cell. Figure 3 shows the effect of sulfuric acid on the nitrate complex. The broad absorption of the nitrate-cerate complex from 250 to 300 mμ is converted to that of the sulfato-cerate complex in 1 N sulfuric acid having ε_{max.} at 320 mμ. The sulfate-cerate absorption generated from the nitrate-cerate (Figure 4) compares favorably with that produced from ceric sulfate in 1 N sulfuric acid. The short wavelength absorption at 240 mμ is primarily due to the displaced nitrate ion.

Figures 5 and 6 show the spectra obtained on (I) unreacted, (II) flowing, and (III) final (after complete reaction) solutions of nitrate-cerate and sulfato-cerate with hydrogen peroxide. In each case, there were no new transient absorption bands observed, and the final spectra were identical to those of the flowing systems (200 cc/min.).

Studies on the superoxide ion are particularly important for understanding the catalytic activity of metal ions. Whereas the oxidation step is reasonably well understood, the reduction step (11) is not. No rate constants for this series of reactions have been reported in the literature as yet.



Our EPR and optical flow studies on this system will be directed toward superoxide reductions of cupric, ferric and other transition metal ions in their high valence states. The nitrate-cerate-hydrogen peroxide reaction will be used as a "superoxide generator".

IV. Container Materials

In view of the complex chemistry associated with the catalytic decomposition of hydrogen peroxide, the best solution to increased stability appears to be to decrease the level of contamination. One method is to start with very pure hydrogen peroxide and the other is to use an inert container. Since previous studies using attenuated total reflection analysis of polymer films indicated that perfluorocarbon polymers were inert toward 90% hydrogen peroxide, containers made from "Teflon" FEP were used for stability tests.

Table IV presents the data on the rate of decomposition of 90% hydrogen peroxide at 66°C in "Teflon" FEP, Pyrex (before and after passivating with nitric acid) and a number of aluminum containers. The striking feature in comparing these data is that the relative rate of decomposition in a "Teflon" FEP container without any special treatment is about equal to that of a carefully passivated aluminum container.

Experiments were also carried out on "Teflon" FEP containers to determine the effect of irradiation. Uniform electron irradiation of a 500 cc. container using a 2 Mev General Electric resonant transformer (beam current 0.5 ma) was achieved by rotating the bottle under the beam at 100 r.p.m. Decomposition rates were determined after each 1 minute dose at 0.5 ma (6.6×10^{-3} kcal/cm²/min.) as shown in Figure 7. The decomposition rate curves for both Pyrex and "Teflon" FEP are presented in Figure 8 and tabulated in Table IV. Although there is marked embrittlement of "Teflon" FEP when irradiated in the presence of oxygen, the decomposition data indicate a decrease in rate from 1.54 to 0.44%/week at 66°C. after a dose of 1.3×10^{-2} kcal/cm².

The effect of electron irradiation on branched perfluorocarbons has been studied in detail by Lovejoy, Bro and Bowers¹¹. In a temperature variation study, they noted that crosslinking of copolymers of tetrafluoroethylene with hexafluoropropylene ("Teflon" FEP) increases with increasing temperature up to 300°C. on electron irradiation in a nitrogen atmosphere. At temperatures below 80°C. and in the presence of oxygen, the formation of peroxy radicals is competitive with the crosslinking reaction and the melt viscosity decreases on irradiation.

Additional irradiation studies are being carried out on "Teflon" FEP containers at elevated temperatures in the absence of oxygen. These will then be tested with 90% hydrogen peroxide to determine decomposition rates.

TABLE S-1

H₂O₂ DECOMPOSITION RATES AT -30°C.SECOND SERIES

| <u>Sample Number</u> | <u>H₂O₂</u> | <u>Manufacturer^b</u> | <u>k^c ppm/day</u> | <u>δ^d</u> | <u>Specific Conductance,^e Micromhos</u> |
|----------------------|-----------------------------------|---------------------------------|------------------------------|--|--|
| 1 | 98 | - | 0.3 | 3.0 | 4.9 |
| 2 | 98 | - | 0.3 | 2.8 | 3.9 |
| 3 | 98 | - | 0.3 | 3.7 | 3.7 |
| 4 | 90 | - | 0.5 | 3.9 | 3.9 |
| 5 | 90 | - | 0.4 | 3.3 | 3.5 |
| 6 | 90 | - | 0.5 | 3.6 | 4.0 |
| 7 | 90 | B | 0.4 | 3.5 | 12.2 |
| 8 | 90 | B | 0.5 | 3.1 | 12.1 |
| 9 | 90 | B | -0.1 | 5.5 | 12.5 |
| 10 | 90 | C | -0.1 | 5.9 | 12.8 |
| 11 | 90 | A | -0.5 | 5.5 | 16.8 |
| 12 | 98 | | -0.6 | 0.6 | 15.5 |

^aActual temperature range was -28.3 to -33.3°C.

^bSamples 1, 2 and 3 were prepared by fractional crystallization and distillation of Du Pont 90% H₂O₂; samples 3, 4 and 5 were prepared by dilution of fractionally crystallized and distilled H₂O₂ with "deionized" water. The remaining samples were commercial H₂O₂. Commercial 90% H₂O₂ was supplied by three manufacturers, designated A, B, and C.

^cCalculated from integrated zero-order rate equation - [H₂O₂] = k Δ t by the method of least squares.

^dStandard deviation of experimentally observed values of - Δ [H₂O₂] from the calculated values.

^eDetermined at end of experiment.

TABLE S-2
H₂O₂ DECOMPOSITION RATES AT 0°C.
SECOND SERIES

| <u>Sample Number</u> | <u>H₂O₂</u> | <u>Manufacturer^b</u> | <u>k^c ppm/day</u> | <u>δ^d</u> | <u>Specific Conductance,^e M. cromhos</u> |
|----------------------|-----------------------------------|---------------------------------|------------------------------|--|---|
| 1 | 98 | - | 0.9 | 2.2 | 4.9 |
| 2 | 98 | - | 0.7 | 1.7 | 3.9 |
| 3 | 98 | - | 0.1 | 0.3 | 3.7 |
| 4 | 90 | - | 0.3 | 1.2 | 3.9 |
| 5 | 90 | - | 0.4 | 1.3 | 3.5 |
| 6 | 90 | - | 1.7 | 3.6 | 4.0 |
| 7 | 90 | B | 0.1 | 1.1 | 12.2 |
| 8 | 90 | B | 0.1 | 1.0 | 12.1 |
| 9 | 90 | B | 0.2 | 1.1 | 12.5 |
| 10 | 90 | C | 3.6 | 7.3 | 12.8 |
| 11 | 90 | A | 3.5 | 7.3 | 16.8 |
| 12 | 98 | | 0.3 | 1.1 | 15.5 |

^aActual temperature range was +1.1 to -5.0°C.

^bSamples 1, 2 and 3 were prepared by fractional crystallization and distillation of Du Pont 90% H₂O₂; samples 3, 4 and 5 were prepared by dilution of fractionally crystallized and distilled H₂O₂ with "deionized" water. The remaining samples were commercial H₂O₂. Commercial 90% H₂O₂ was supplied by three manufacturers, designated A, B and C.

^cCalculated from integrated zero-order rate equation - $\Delta[\text{H}_2\text{O}_2] = k \Delta t$ by the method of least squares.

^dStandard deviation of experimentally observed values of $-\Delta[\text{H}_2\text{O}_2]$ from the calculated values.

^eDetermined at end of experiment.

TABLE I

RATE CONSTANTS OF HYDROXYL RADICALS WITH HALOGEN IONS

| <u>Reactant</u> | <u>pH</u> | <u>k (M⁻¹ sec⁻¹)</u> | <u>Reference</u> |
|-----------------|-----------|--|------------------|
| Cl ⁻ | 0 | 4 x 10 ⁹ | 12 |
| | 0 | 4 x 10 ⁹ | 2 |
| | 3 | 2 x 10 ⁷ | 2 |
| Br ⁻ | 0 | 1.6 x 10 ¹⁰ | 12 |
| | 0-2 | 3.6 x 10 ¹⁰ | 13 |
| | 7 | 1.3 x 10 ⁸ | 14 |
| | 7 | 1.3 x 10 ⁹ | 15 |
| | 7 | 1.3 x 10 ⁸ | 16 |
| I ⁻ | 7 | 1.6 x 10 ⁹ | 17 |
| | 7 | ~1.2 x 10 ⁹ | 18 |

TABLE II

RATE CONSTANTS OF HYDROXYL RADICALS WITH METAL IONS

| <u>Reactant</u> | <u>pH</u> | <u>k(M⁻¹ sec⁻¹)</u> | <u>Reference</u> |
|-----------------------------------|-----------|---|------------------|
| Fe ⁺² | 1 | 3.0 x 10 ⁸ | 19 |
| | 0 | > 10 ⁸ | 20 |
| | 1.57 | 3.2 x 10 ⁸ | 21 |
| | 2.0 | 2.6 x 10 ⁸ | 22 |
| | 2.1 | 2.5 x 10 ⁸ | 21 |
| | 1.0 | 3.2 x 10 ⁸ | 23 |
| Fe(CN) ₆ ⁺⁴ | 2.5-10.5 | 2.1 x 10 ⁹ | 24 |
| Sn ⁺² | 0.1 | 2 x 10 ⁹ | 25 |
| Tl ⁺¹ | 0.1 | 8.5 x 10 ⁹ | 26 |
| Ce ⁺³ | 0.1 | 2.2 x 10 ⁸ | 26, 27 |

TABLE III

RATE CONSTANTS OF HYDROXYL RADICALS WITH VARIOUS ANIONS

| <u>Reactant</u> | <u>pH</u> | <u>k(M⁻¹ sec⁻¹)</u> | <u>Reference</u> |
|------------------------------|-----------|---|------------------|
| CO ₃ ⁼ | 7 | 8 x 10 ⁷ | 16 |
| CNS ⁻ | 7 | 1.3 x 10 ⁹ | 16 |
| OH ⁻ | | 3.6 x 10 ⁸ | 28,29 |
| NC ⁻ | 7 | 2.5 x 10 ⁹ | 30 |
| SO ₃ ⁼ | 7 | 1.2 x 10 ⁹ | 16 |
| HSO ₃ | 7 | 2.1 x 10 ⁹ | 16 |
| HSO ₄ | 0.1 | 3.3 x 10 ⁷ | 25 |

TABLE IV

STABILITY OF 90% HYDROGEN PEROXIDE IN VARIOUS CONTAINERS

| <u>Sample Container</u> | <u>Rate of Decomposition per Week at 66°C. (% of total)</u> |
|---|---|
| Aluminum alloys* | |
| Alcoa 1060 | 1.5 |
| Alcoa 1100 | 3.0 |
| Alcoa 1160 | 1.5 |
| Alcoa 1260 | 1.5 |
| Passivated Pyrex** | 1.0 (approx.) |
| Unpassivated Pyrex*** | 4.7 |
| Passivated Pyrex*** | 1.06 |
| Unpassivated "Teflon" FEP*** | 1.54 |
| Irradiated "Teflon" FEP*** (1.3×10^{-2} kcal/cm ²) | 0.44 |

*Data taken from Bulletin No. 104, Becco Chemical Division of Food Machinery and Chemical Corporation, 1959.

**Data taken from Bulletin No. SD-53, Supplement B, p. 23, Manufacturing Chemists Association, Inc., Chemical Data Sheet on Hydrogen Peroxide, 1961.

***Data from this report, see Figure 8.

FIGURE S-1

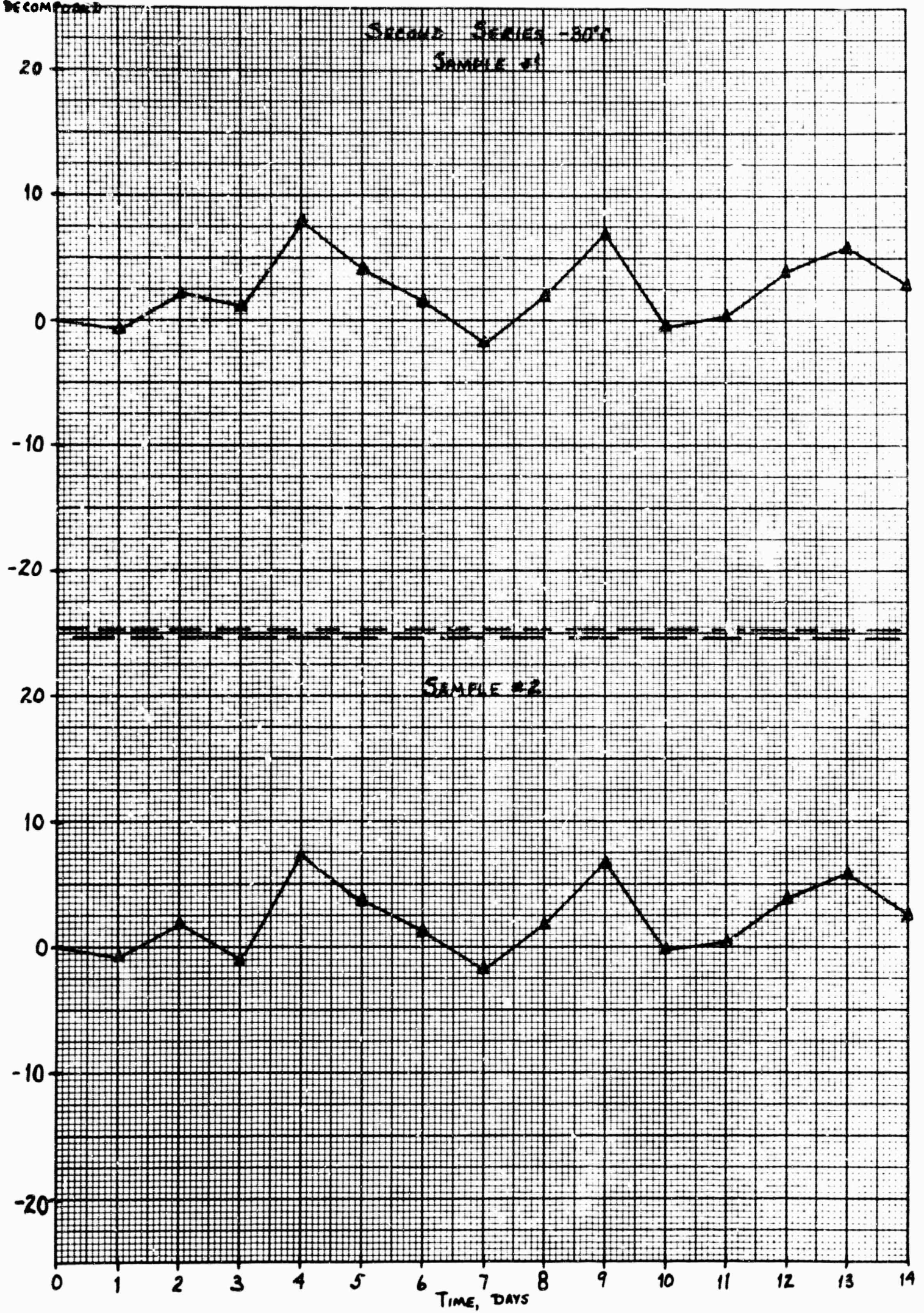
H₂O₂ DECOMPOSITION RATES AT -30°C.

SECOND SERIES

NOTES

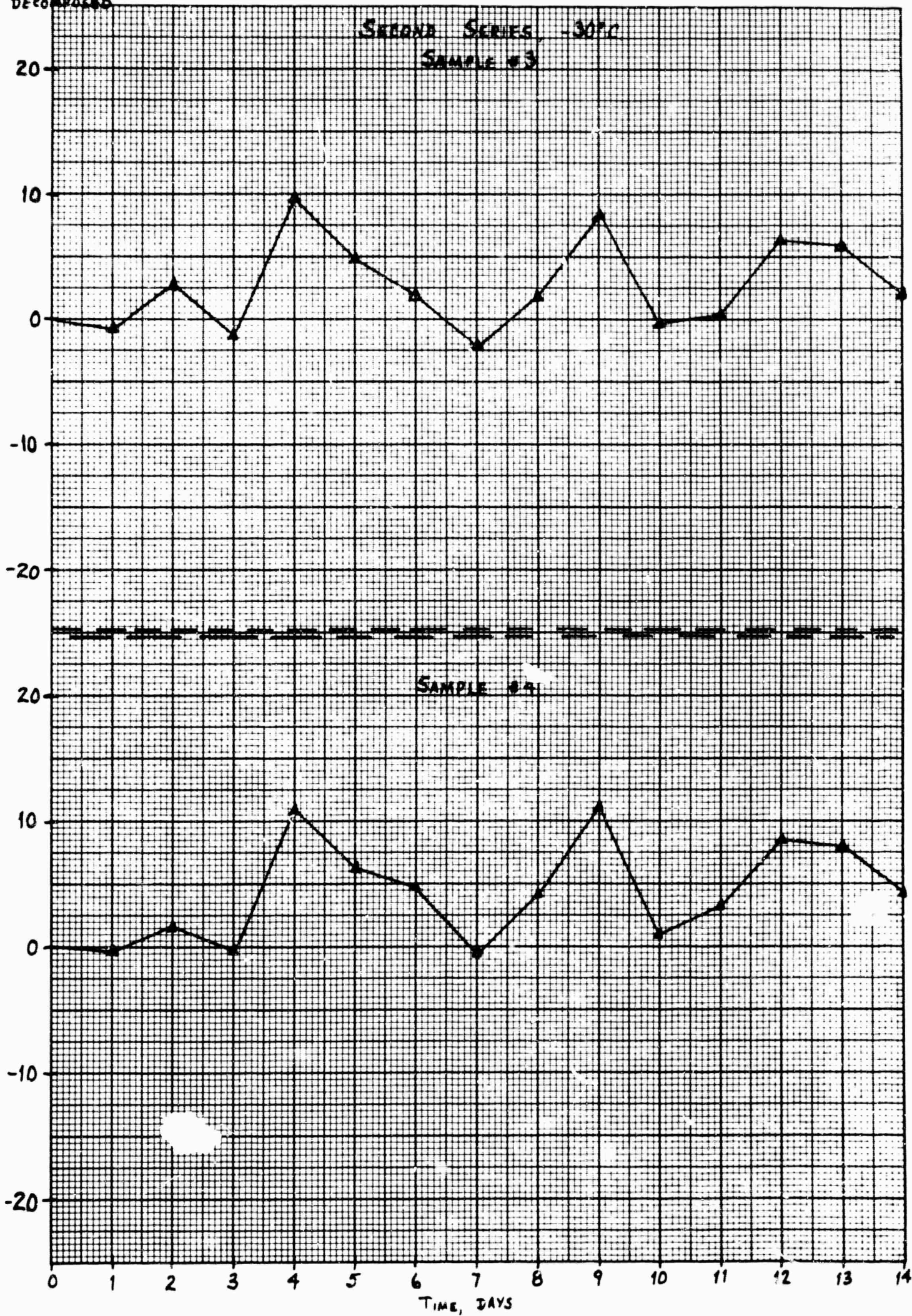
1. This Figure consists of 12 parts, which follow.
2. Identification of samples
 - a. #1, #2 and #3 - unstabilized 98% H₂O₂
 - b. #4, #5 and #6 - unstabilized 90% H₂O₂
 - c. #7, #8 and #9 - commercial 90% H₂O₂, manufacturer B
 - d. #10 - commercial 90% H₂O₂, manufacturer C
 - e. #11 - commercial 90% H₂O₂, manufacturer A
 - f. #12 - commercial 98% H₂O₂
3. The plotted are "cumulative" curves which show the apparent total amount (in ppm. or original sample) decomposed at any given time.

ppm
H₂O₂
DECOMPOSED

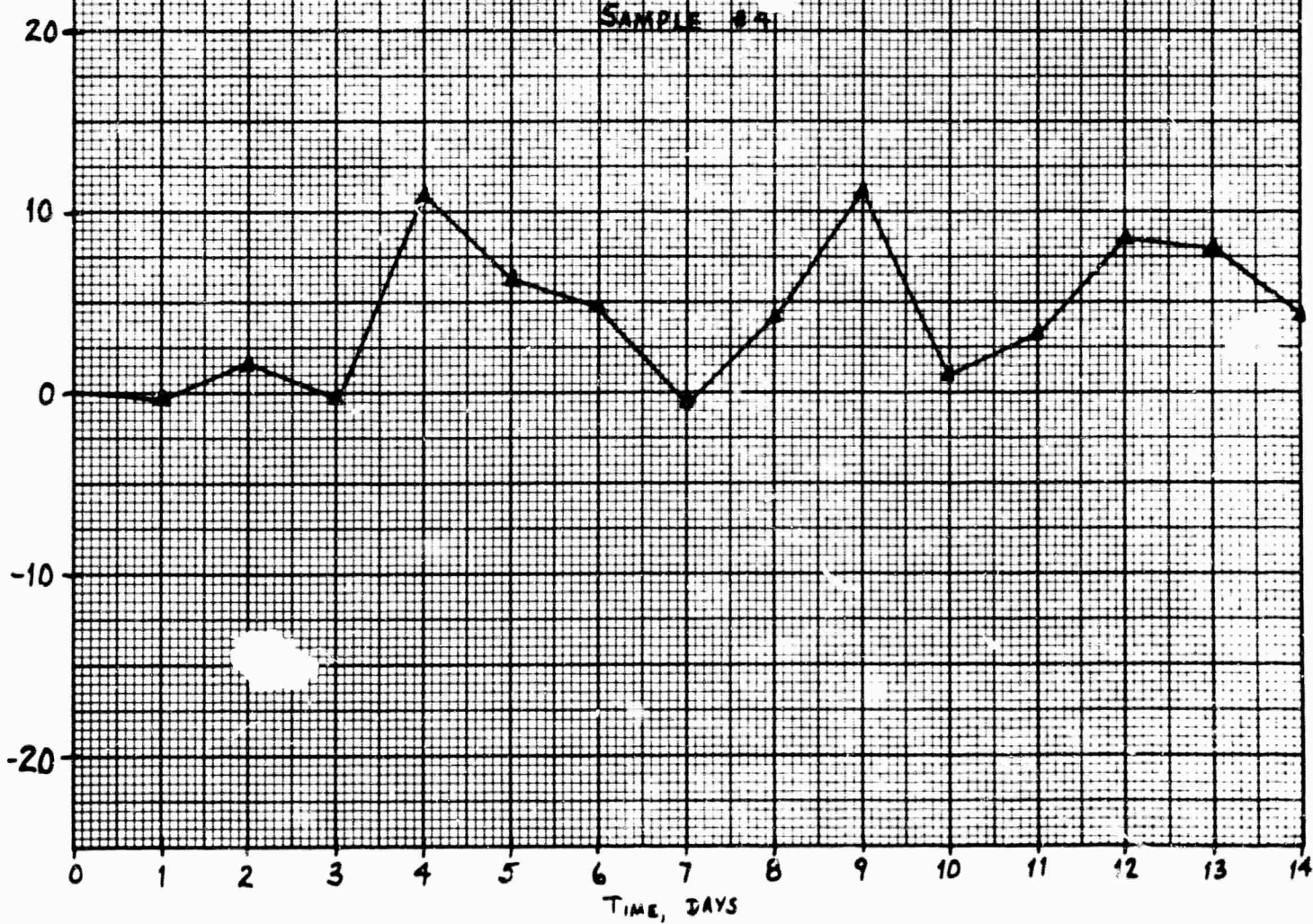


ppm
 H_2O_2
DECOMPOSED

SECOND SERIES, -30°C
SAMPLE #3

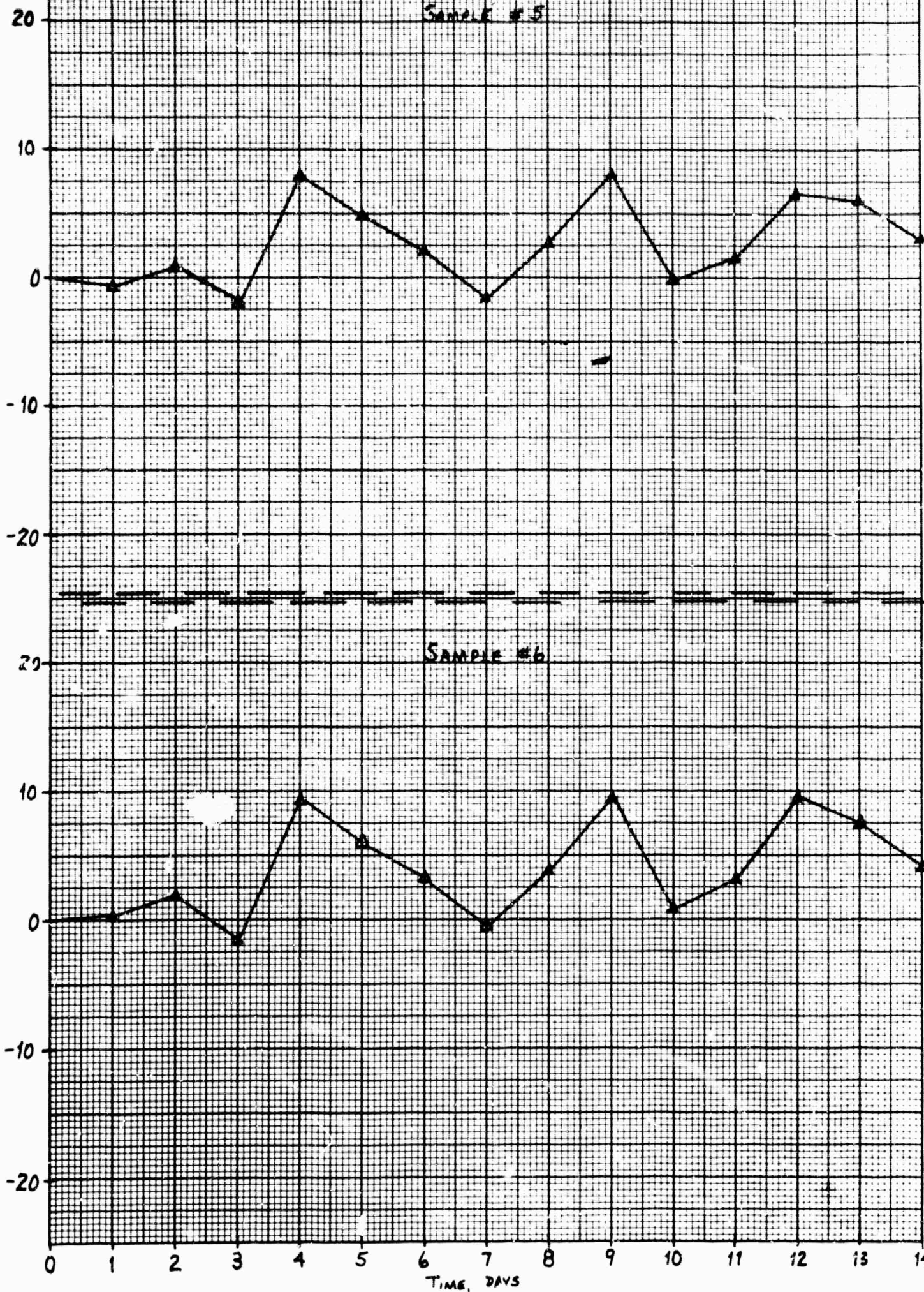


SAMPLE #4

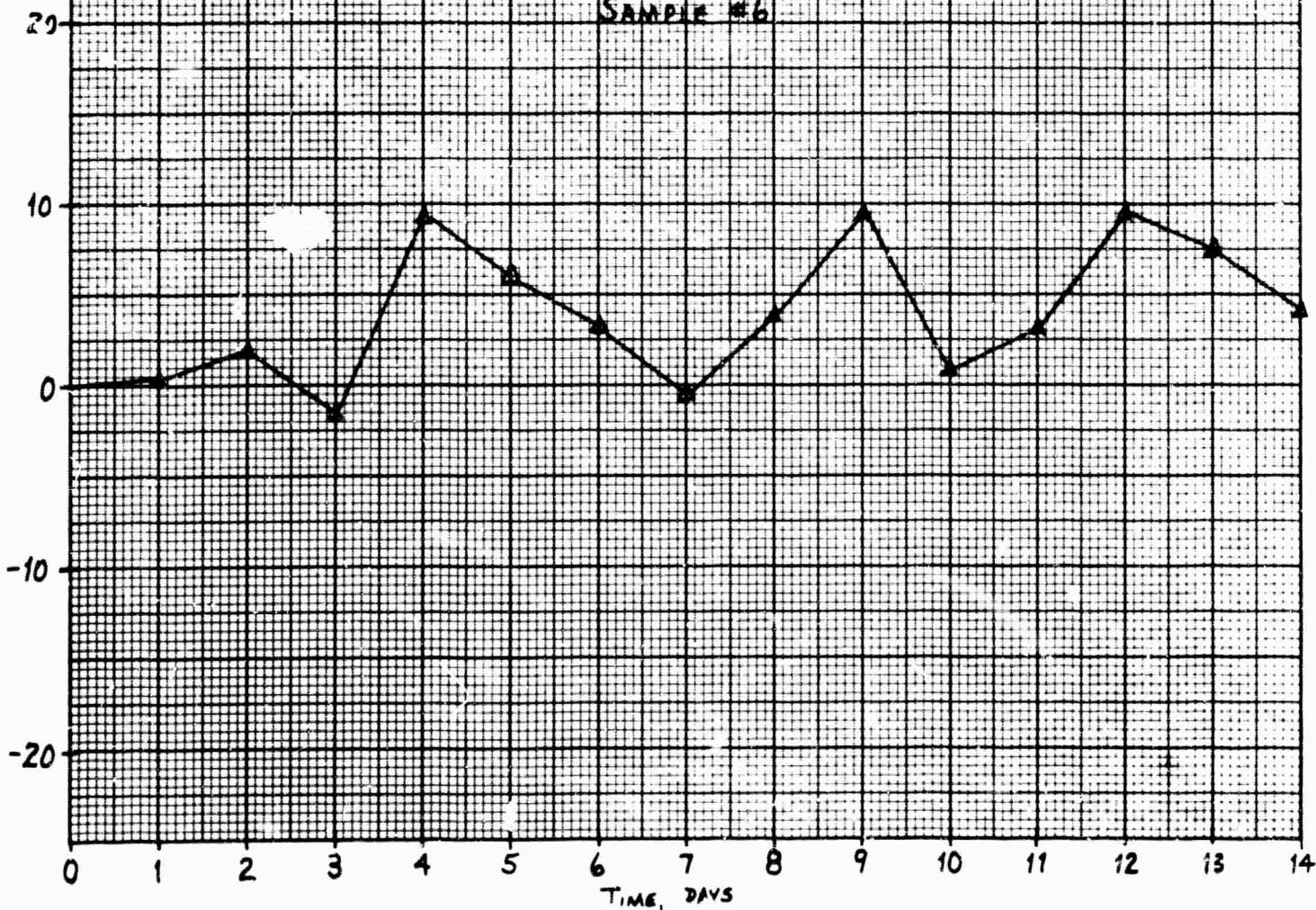


ppm
 H_2O_2
DECOMPOSED

SECOND SERIES - 20°C
SAMPLE #5



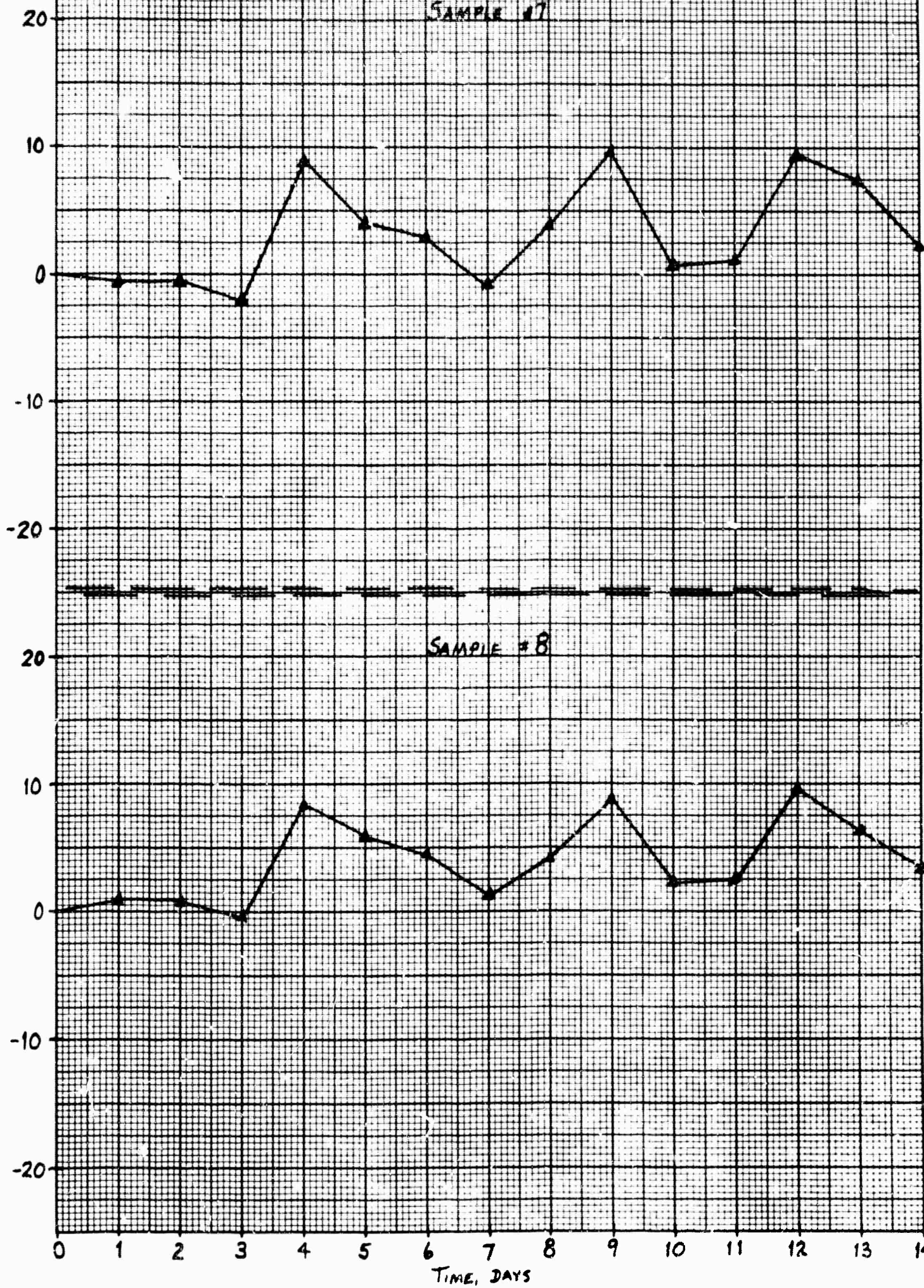
SAMPLE #6



PPM
 H_2O_2
DECOMPOSED

SECOND SERIES - 30%

SAMPLE #7



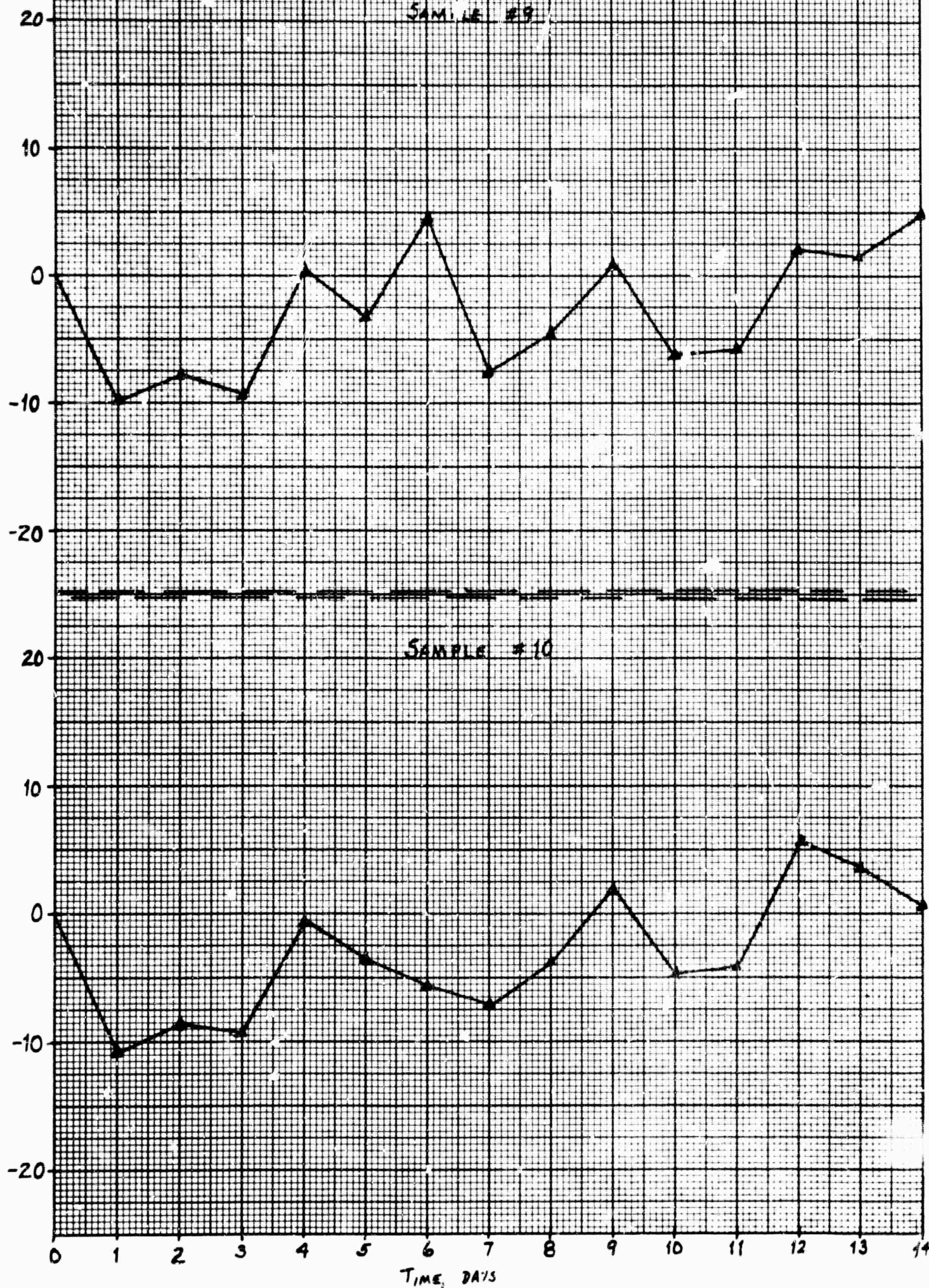
TIME, DAYS

ppm
 H_2O_2

DECOMPOSED

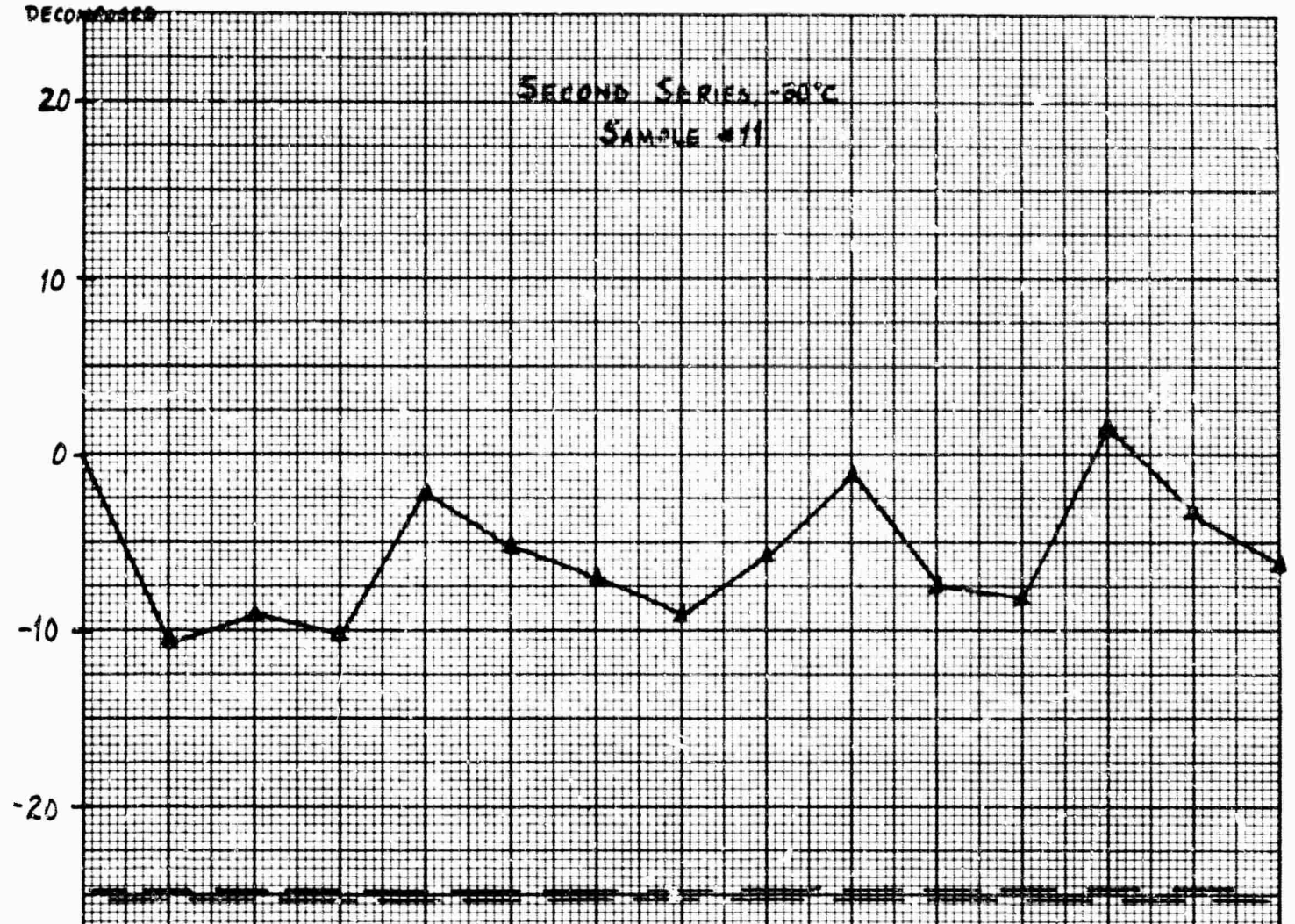
SECOND SERIES, 3015

SAMPLE #9



ppm
H₂O₂
DECOMPOSED

SECOND SERIES -60°C
SAMPLE #11



SAMPLE #12

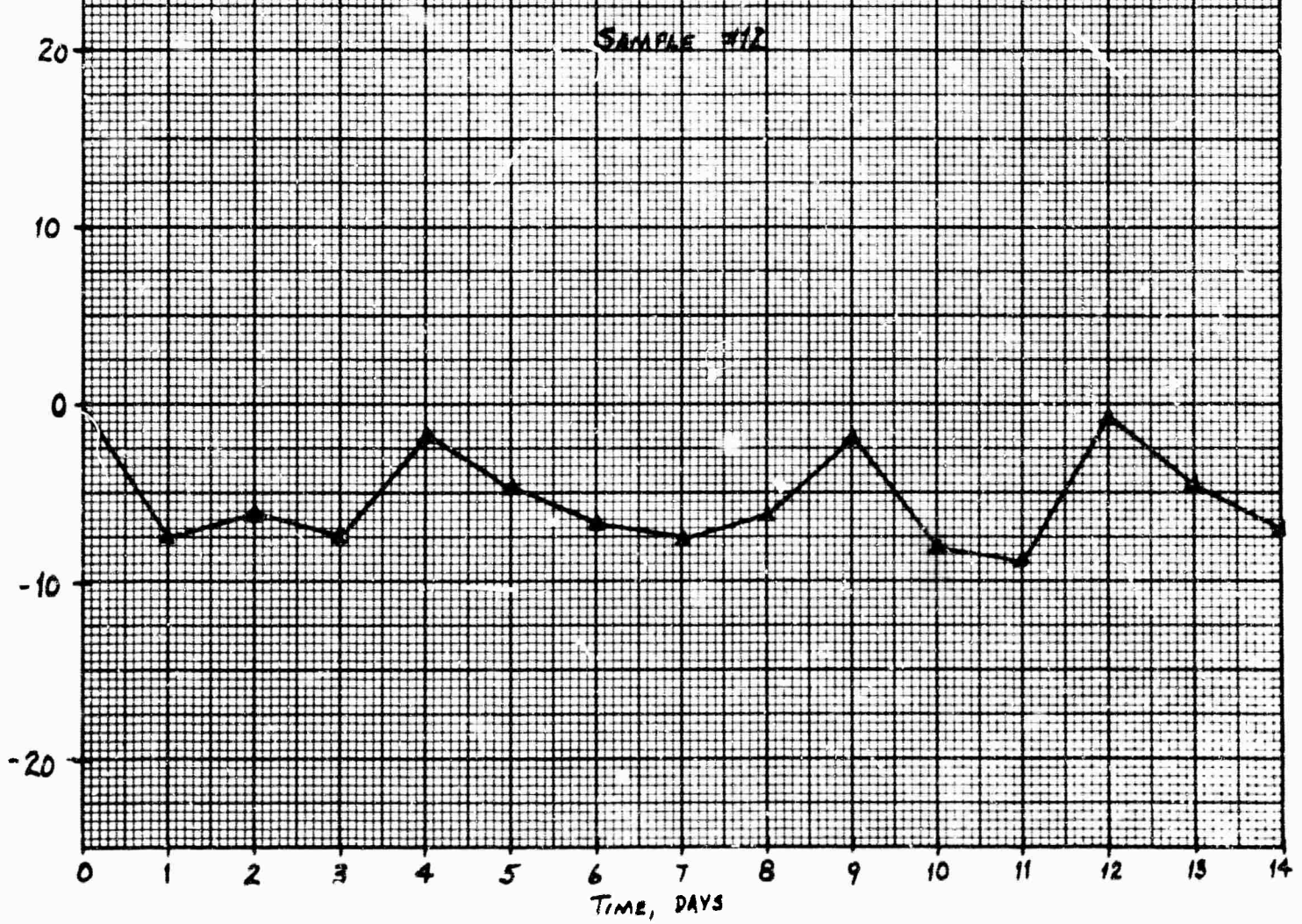


FIGURE S-2

H₂O₂ DECOMPOSITION RATES AT 0°C.

SECOND SERIES

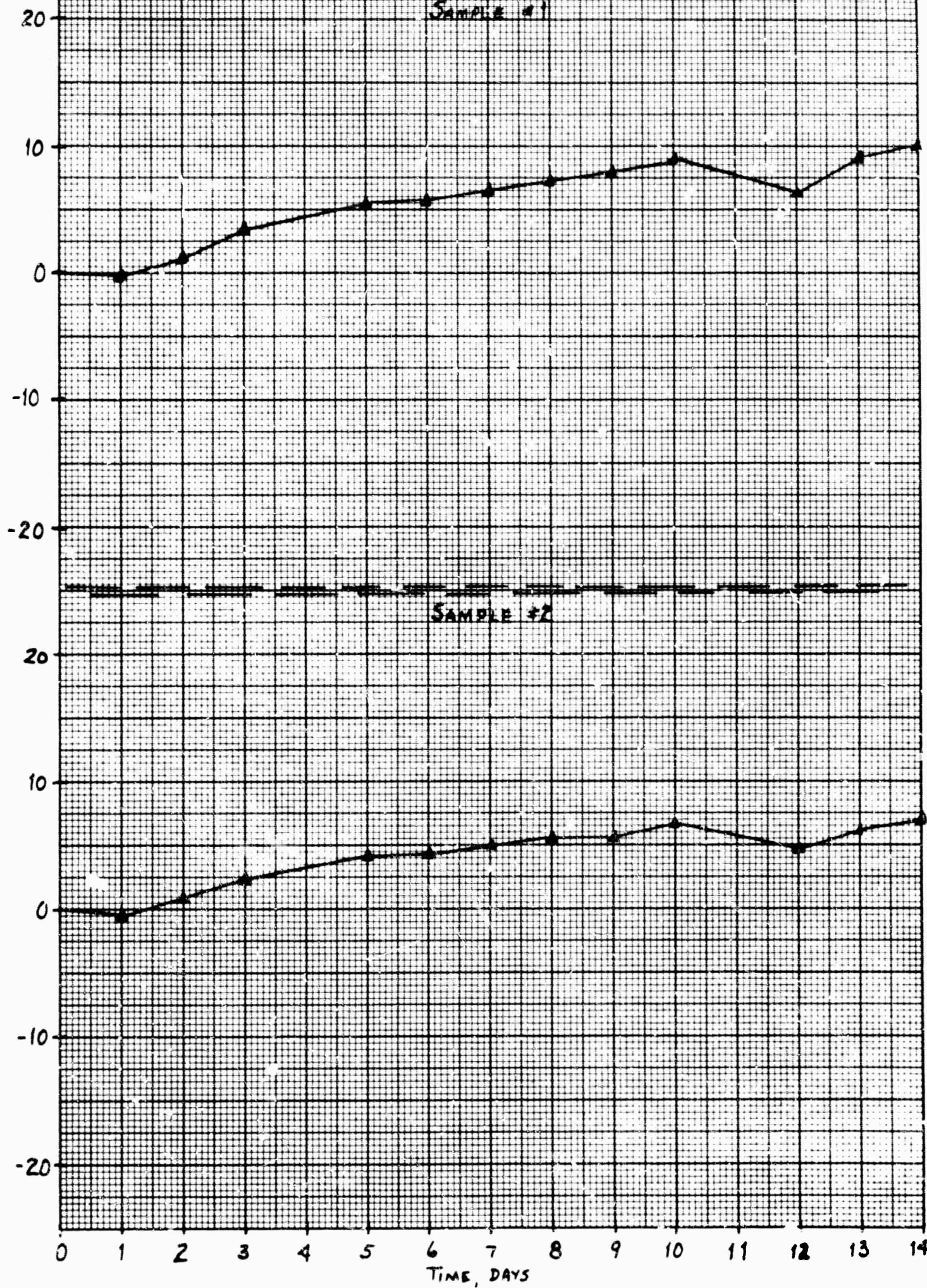
NOTES

1. This Figure consists of 12 parts, which follow.
2. Identification of samples
 - a. #1, #2 and #3 - unstabilized 98% H₂O₂
 - b. #4, #5 and #6 - unstabilized 90% H₂O₂
 - c. #7, #8 and #9 - commercial 90% H₂O₂, manufacturer B
 - d. #10 - commercial 90% H₂O₂, manufacturer C
 - e. #11 - commercial 90% H₂O₂, manufacturer A
 - f. #12 - commercial 98% H₂O₂
3. The curves plotted are "cumulative" curves which show the apparent total amount (in ppm or original sample) decomposed at any given time.

PPM
 H_2O_2
DECOMPOSED

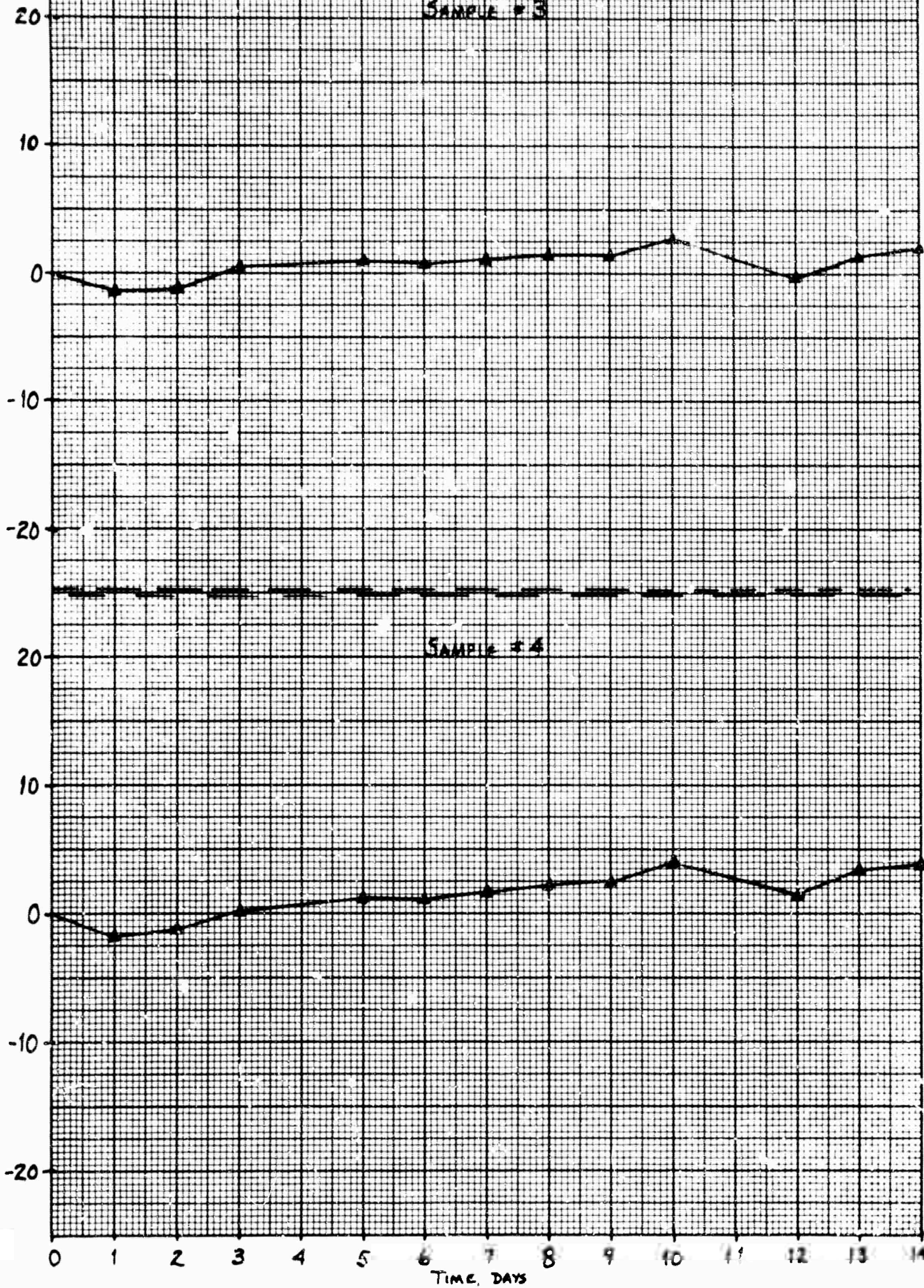
SECOND SERIES, 0°C

SAMPLE #1



PFM
H₂O₂
DECOMPOSED

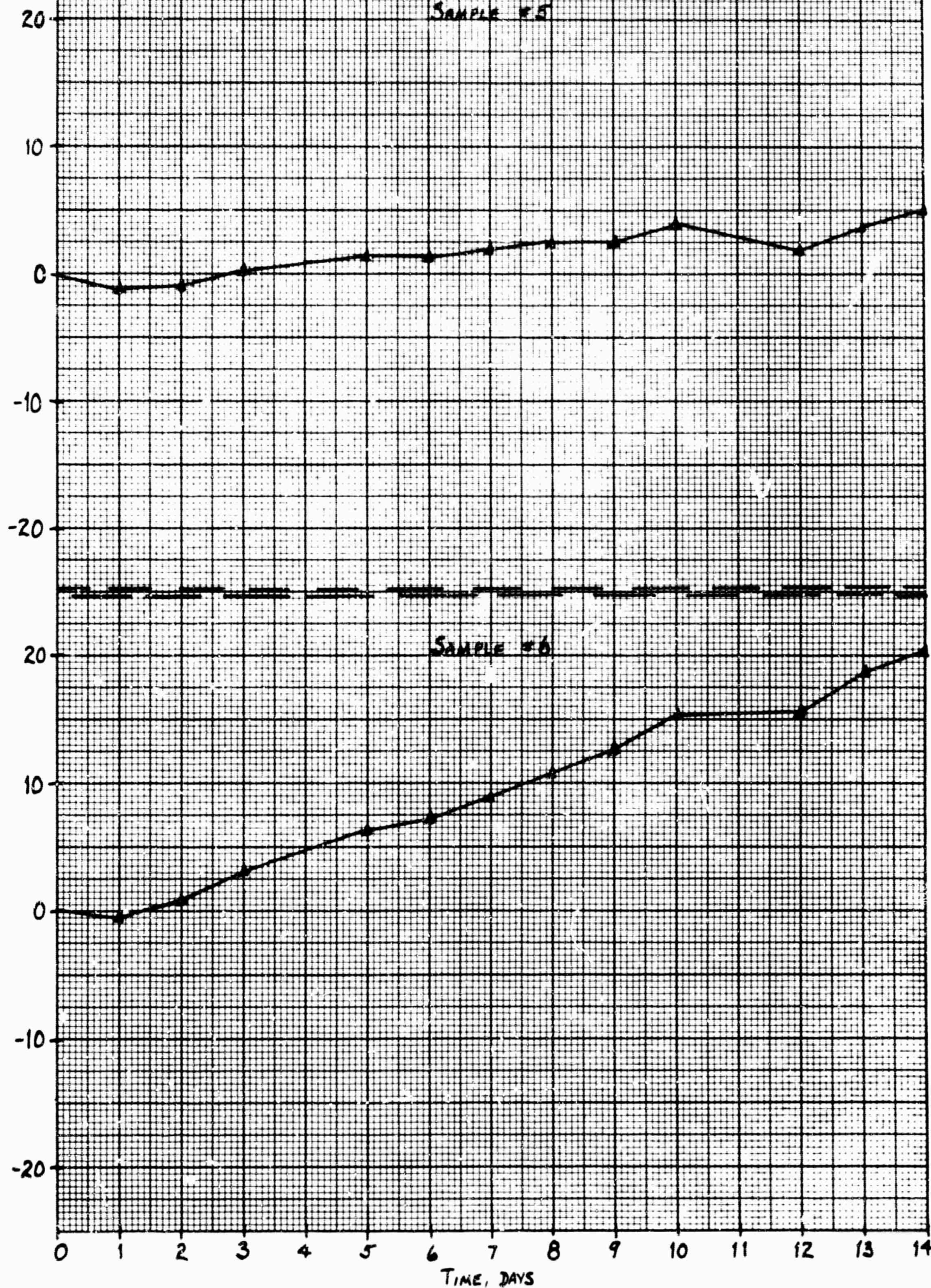
SECOND SERIES 0°C
SAMPLE #3



ppm
 H_2O_2
DECOMPOSED

SECOND SERIES 0°C.

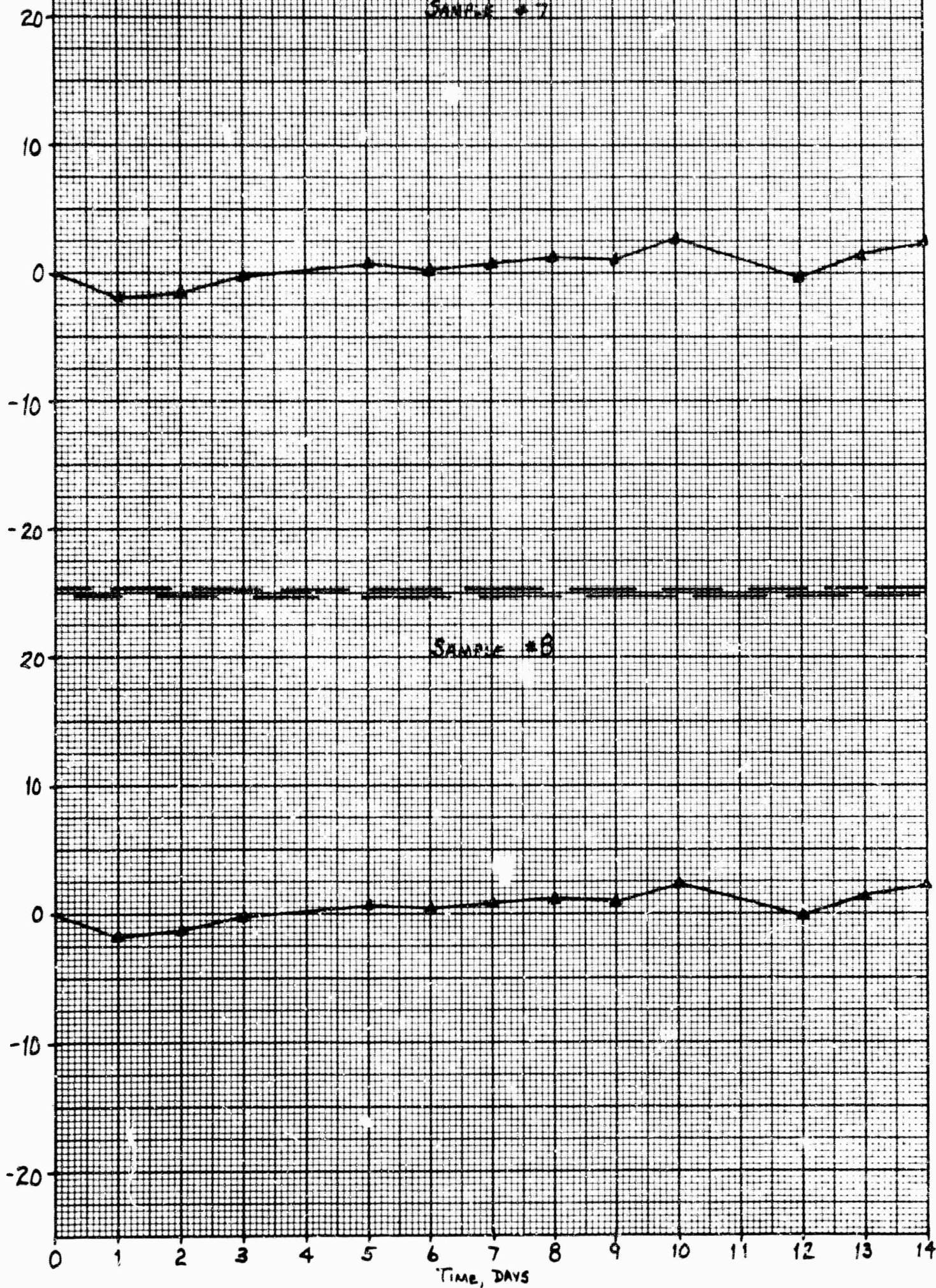
SAMPLE #5



H₂O₂
DECOMPOSED

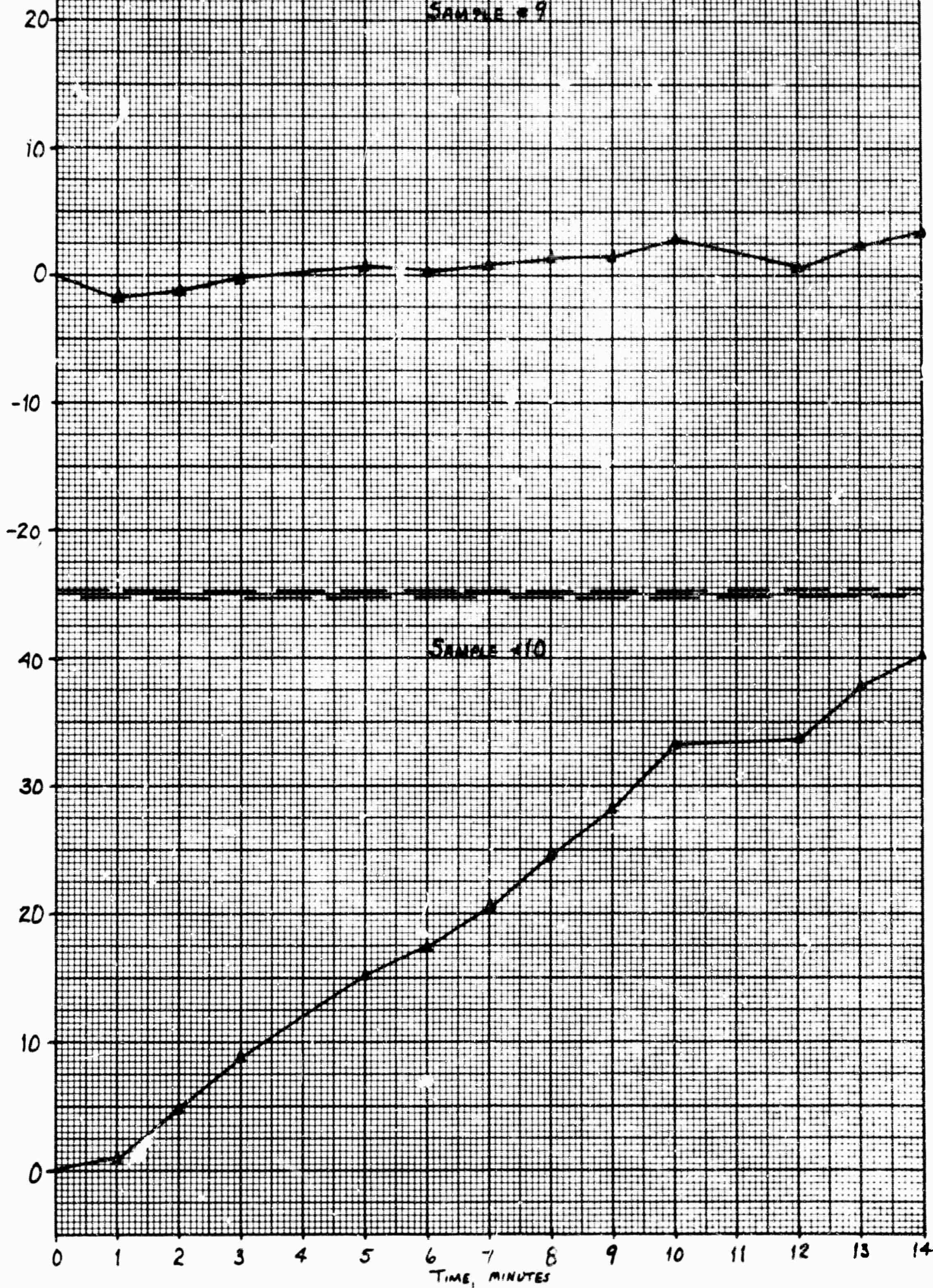
SECOND SERIES, 0°C

SAMPLE #7



H₂O₂
DECOMPOSE

SECOND SERIES, 0°C
SAMPLE #9



H₂O₂
DECOMPOSED

SECOND SERIES, 0°C

SAMPLE # 11

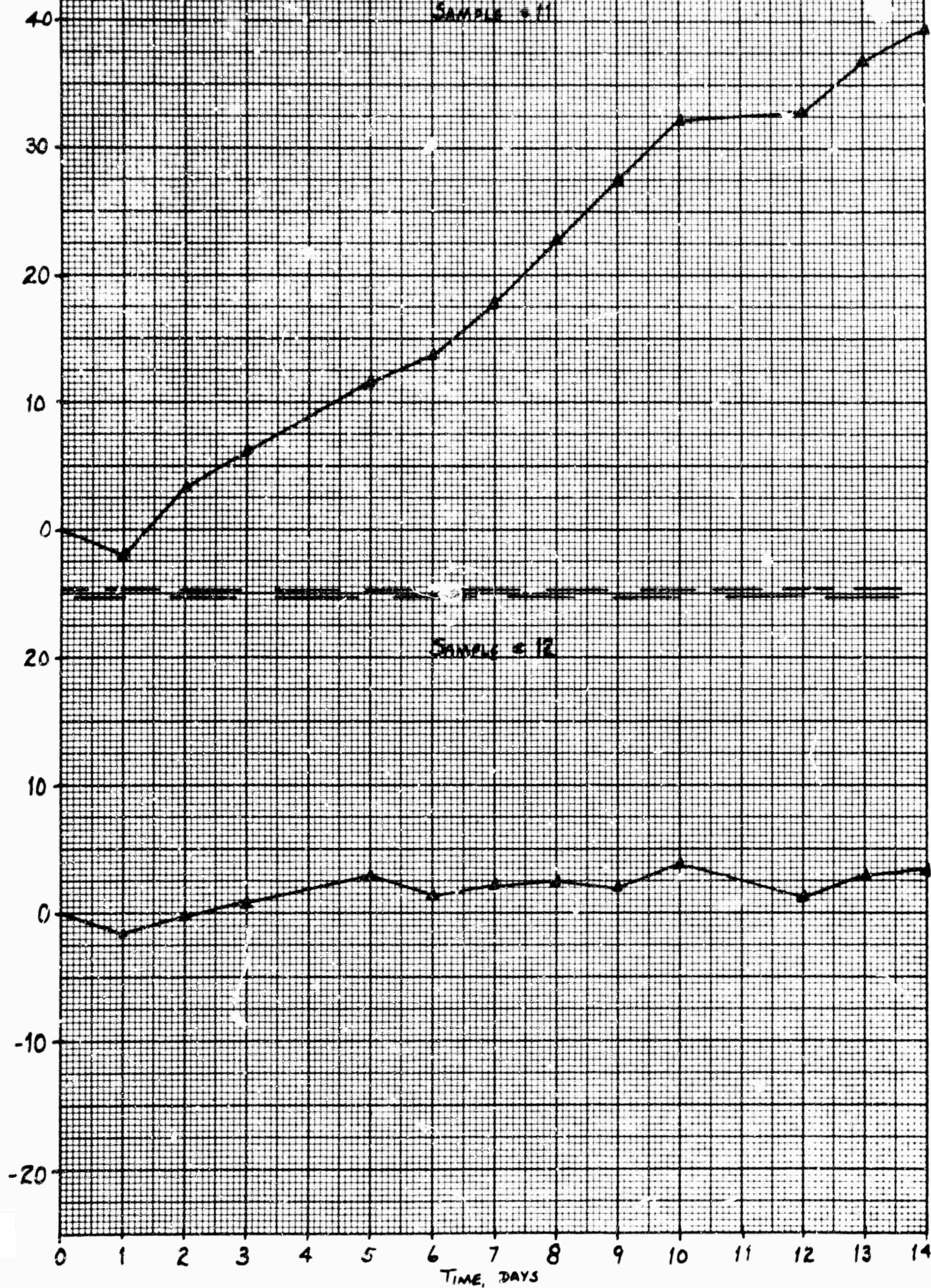
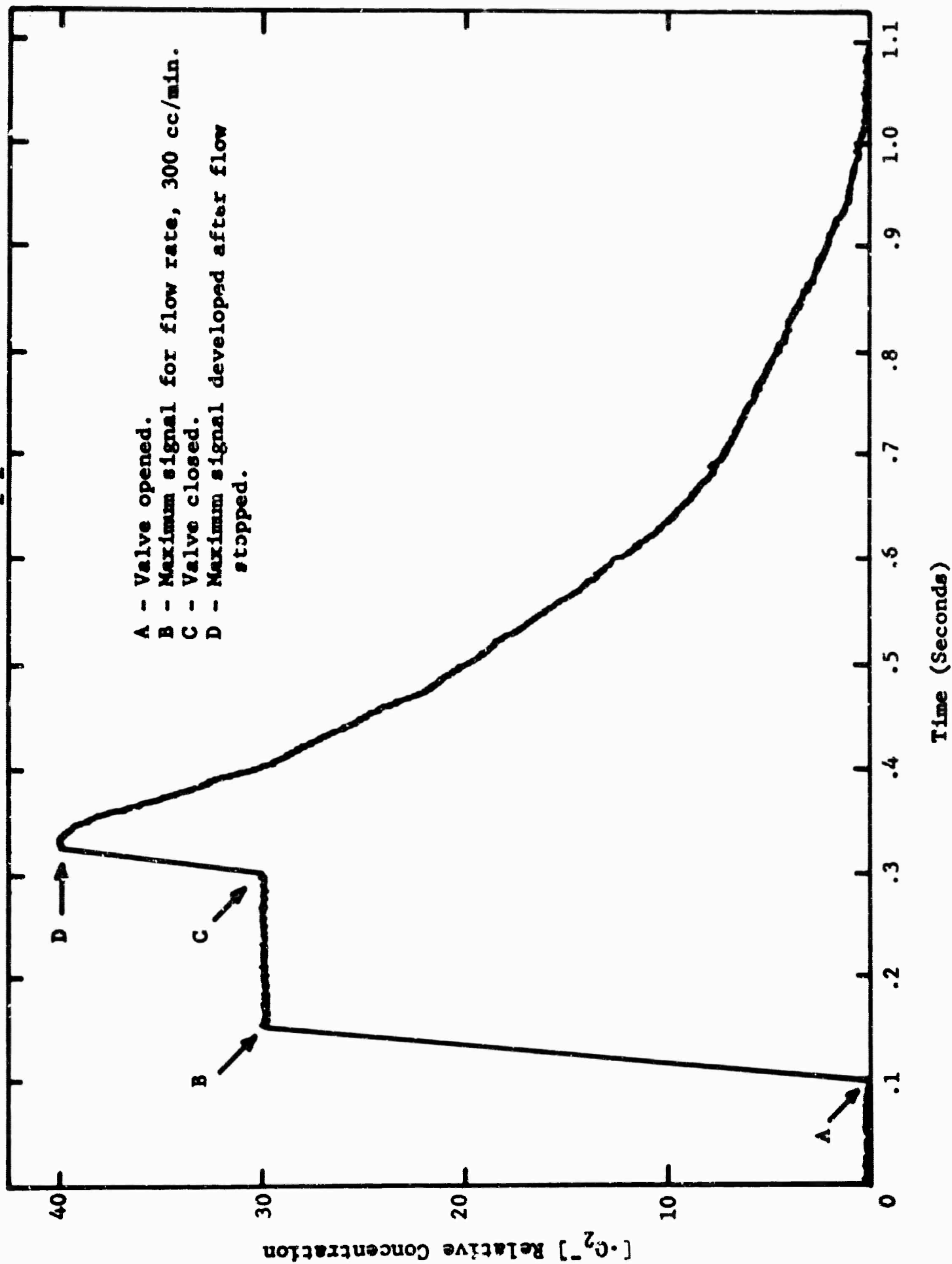


FIGURE 1
Stopped Flow Studies on $Ti^{+3} - H_2O_2$ Reaction



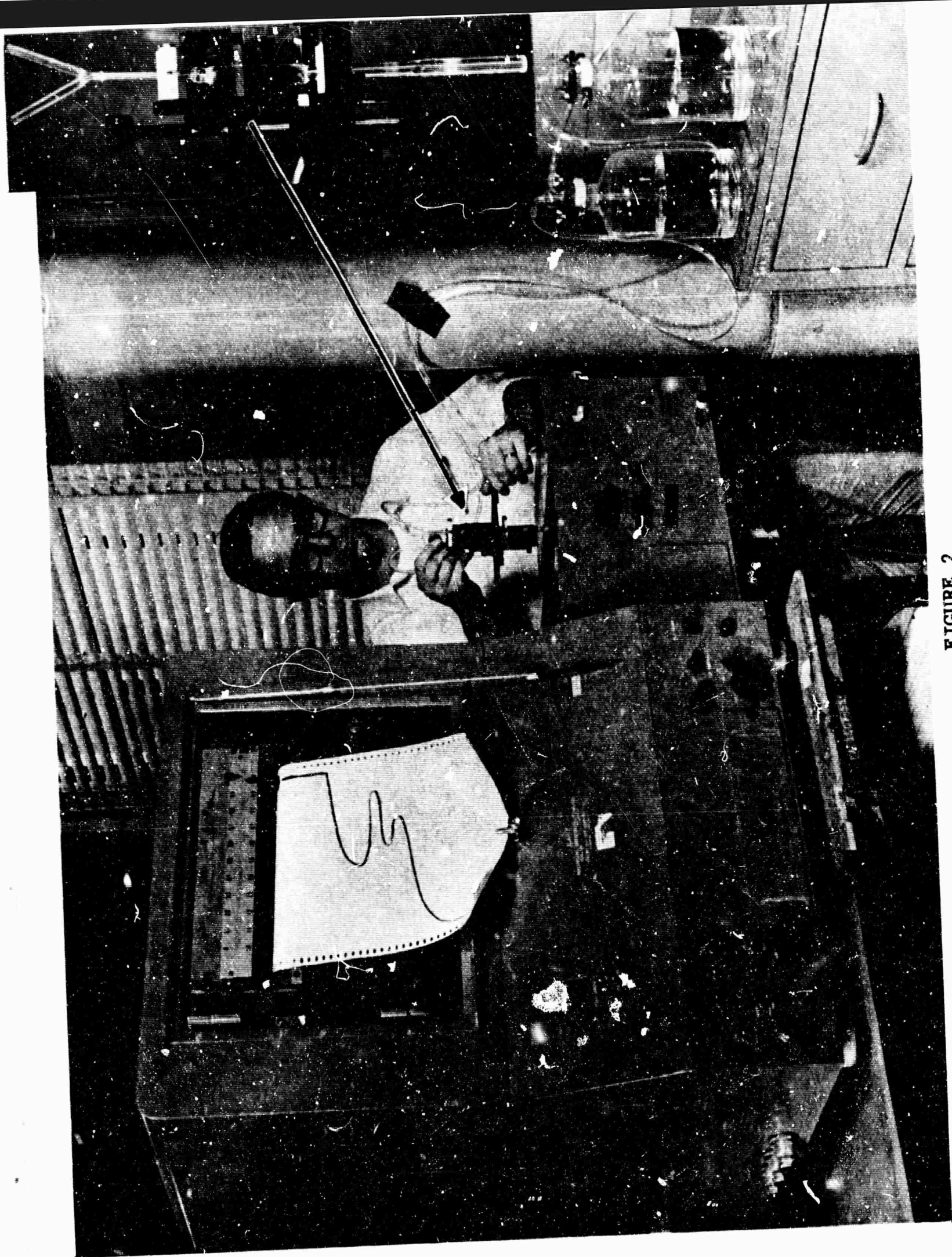


FIGURE 2

FIGURE 2

Flow Cell for Optical Absorption Spectra

FIGURE 3

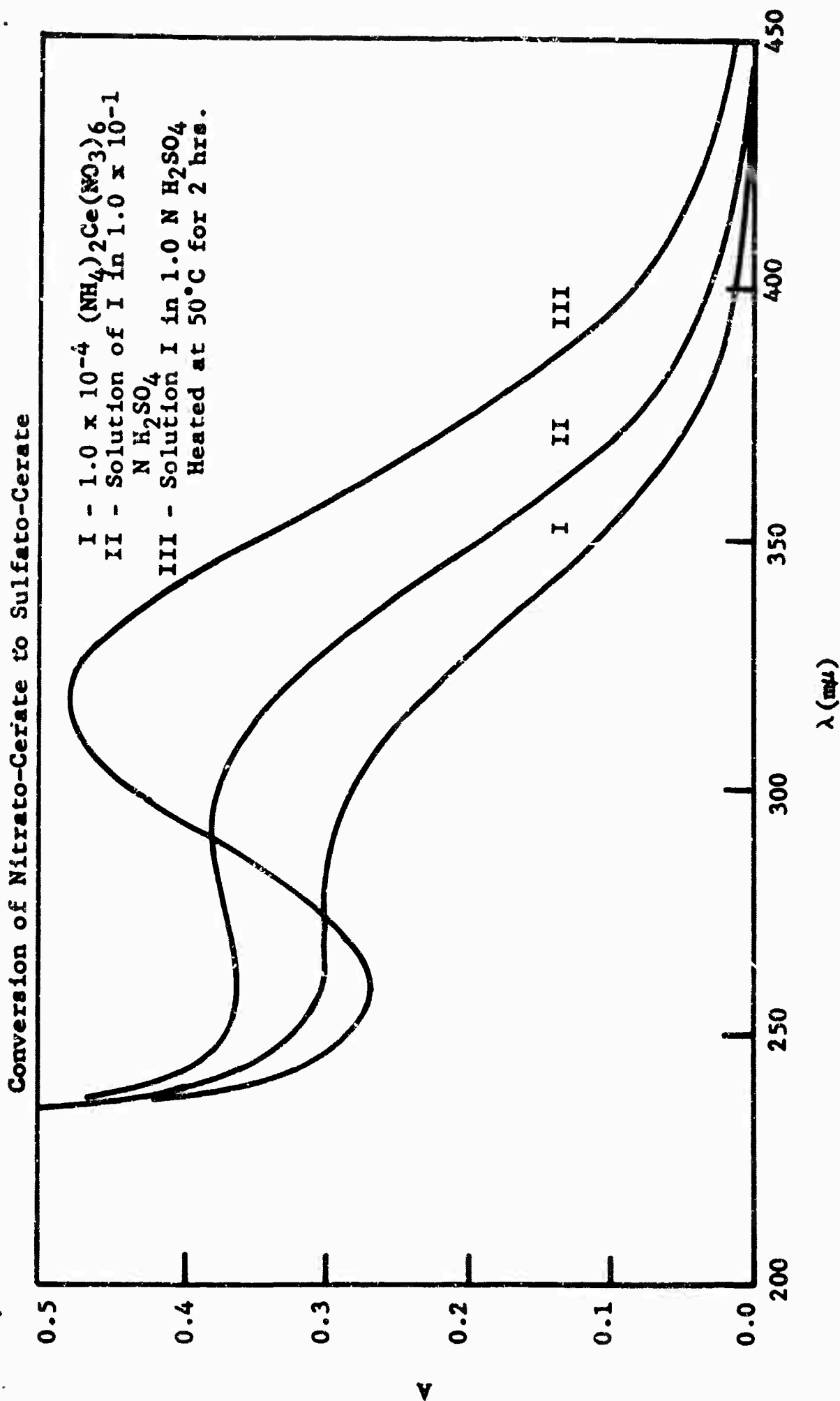


FIGURE 4

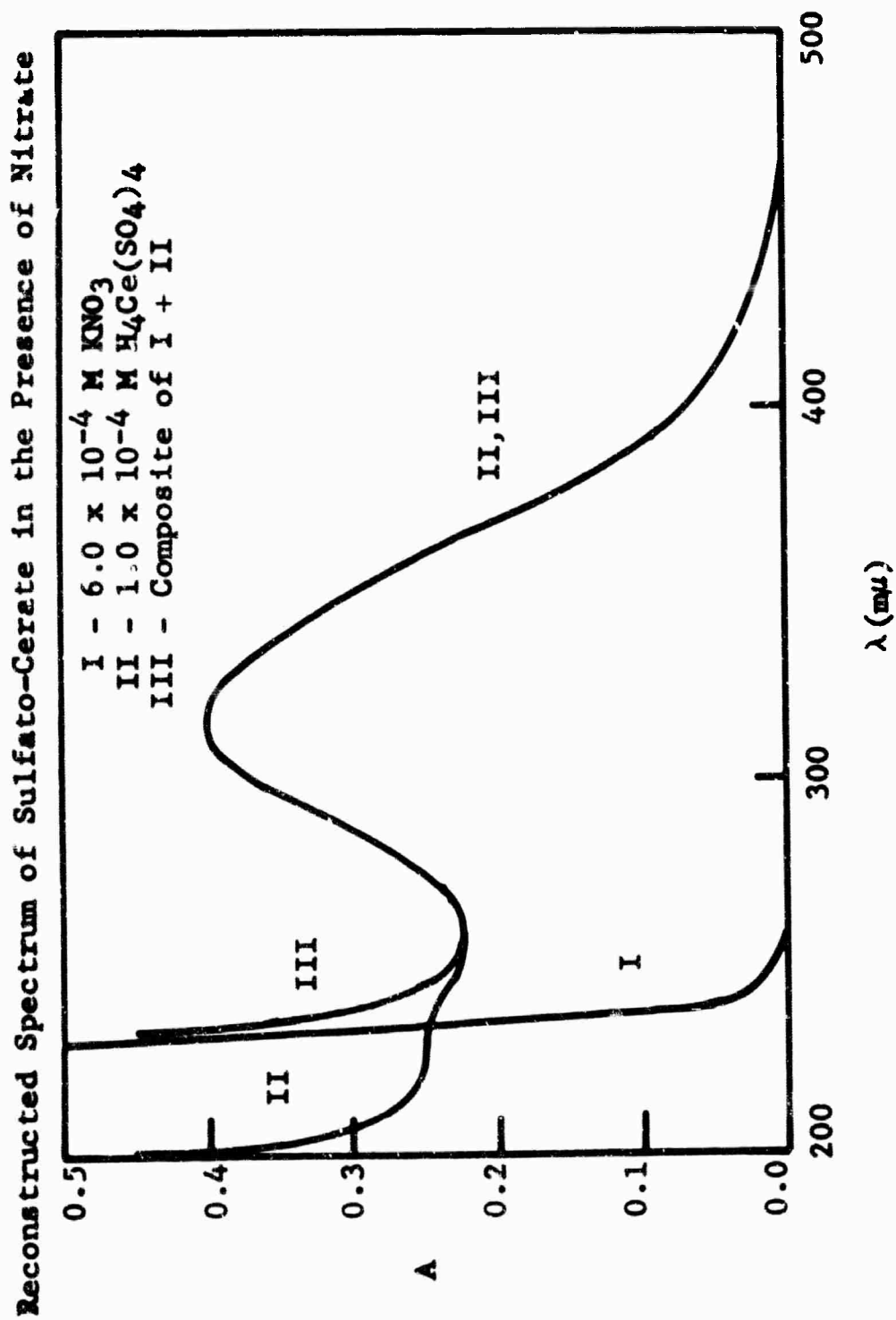


FIGURE 5

Optical Flow Studies on the Nitrate-Cerate, Hydrogen Peroxide Reaction

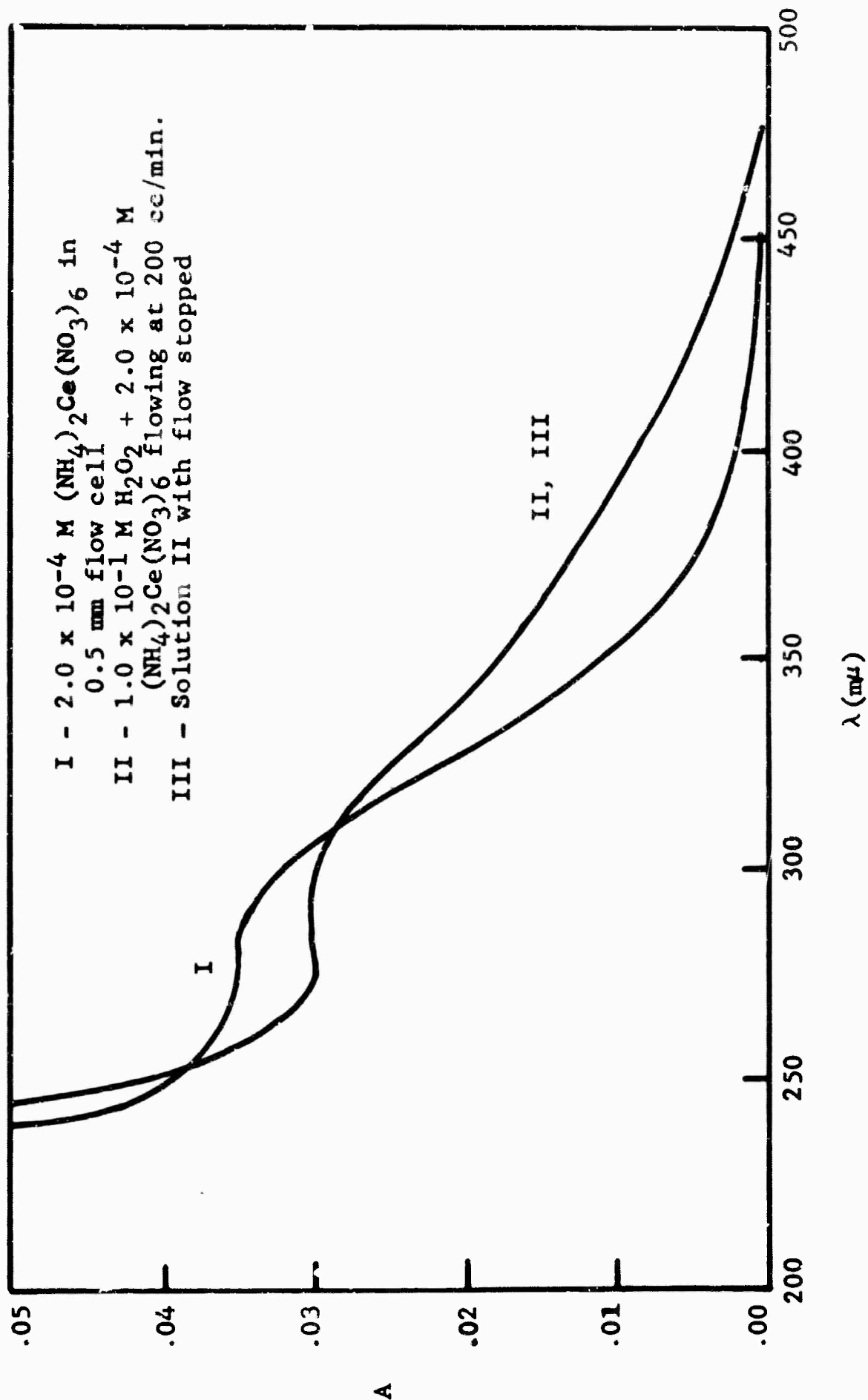


FIGURE 6

Optical Flow Studies on the Sulfato-Cerate, Hydrogen Peroxide Reaction

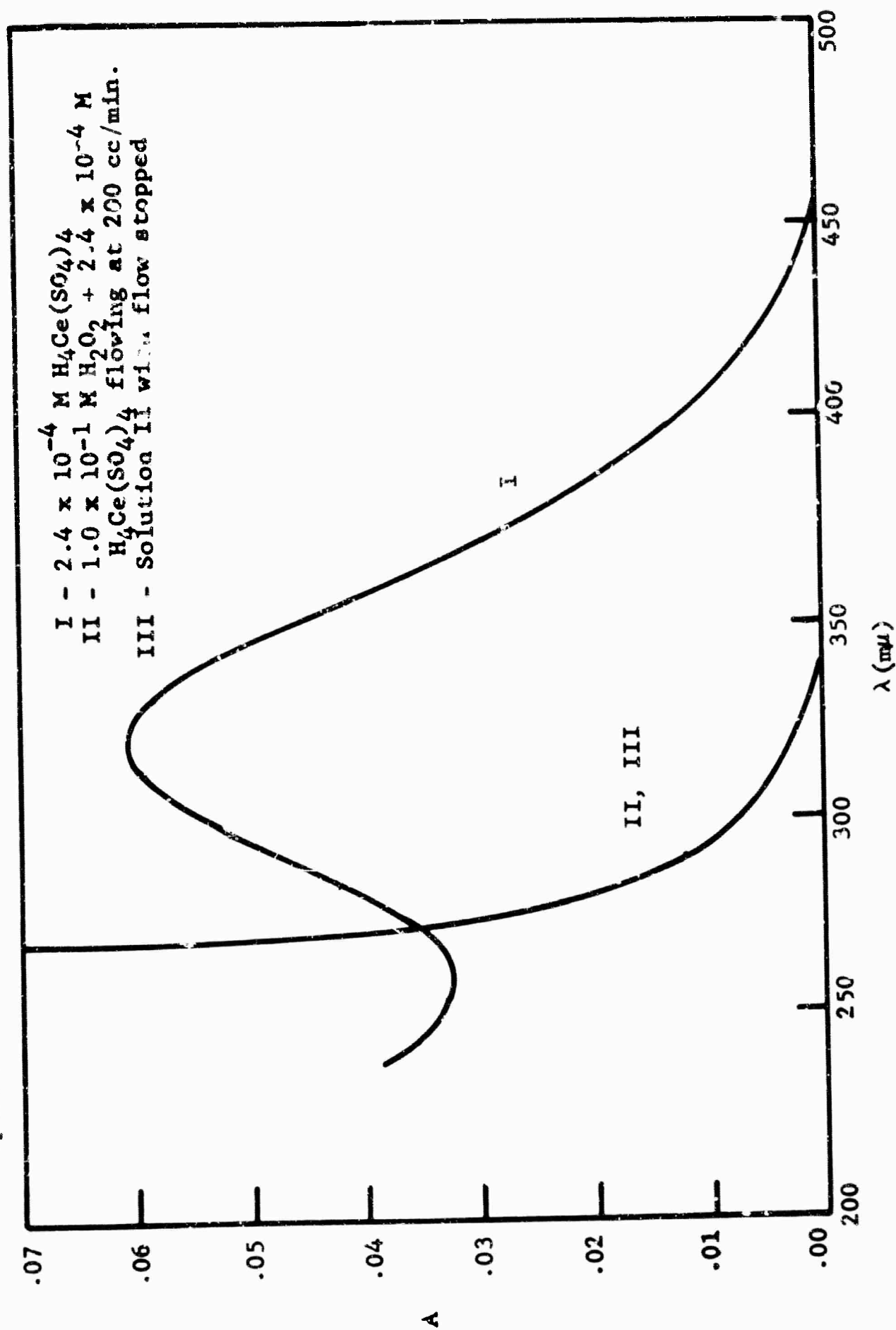


FIGURE 7

Effect of Electron Irradiation of "Teflon" FEP Container on the Decomposition
Rate of Hydrogen Peroxide

Sample - 383 ml of 90% H_2O_2 in a "Teflon" FEP bottle at 66°C

Dose Rate - 6.6×10^{-3} kcal/cm²/min.

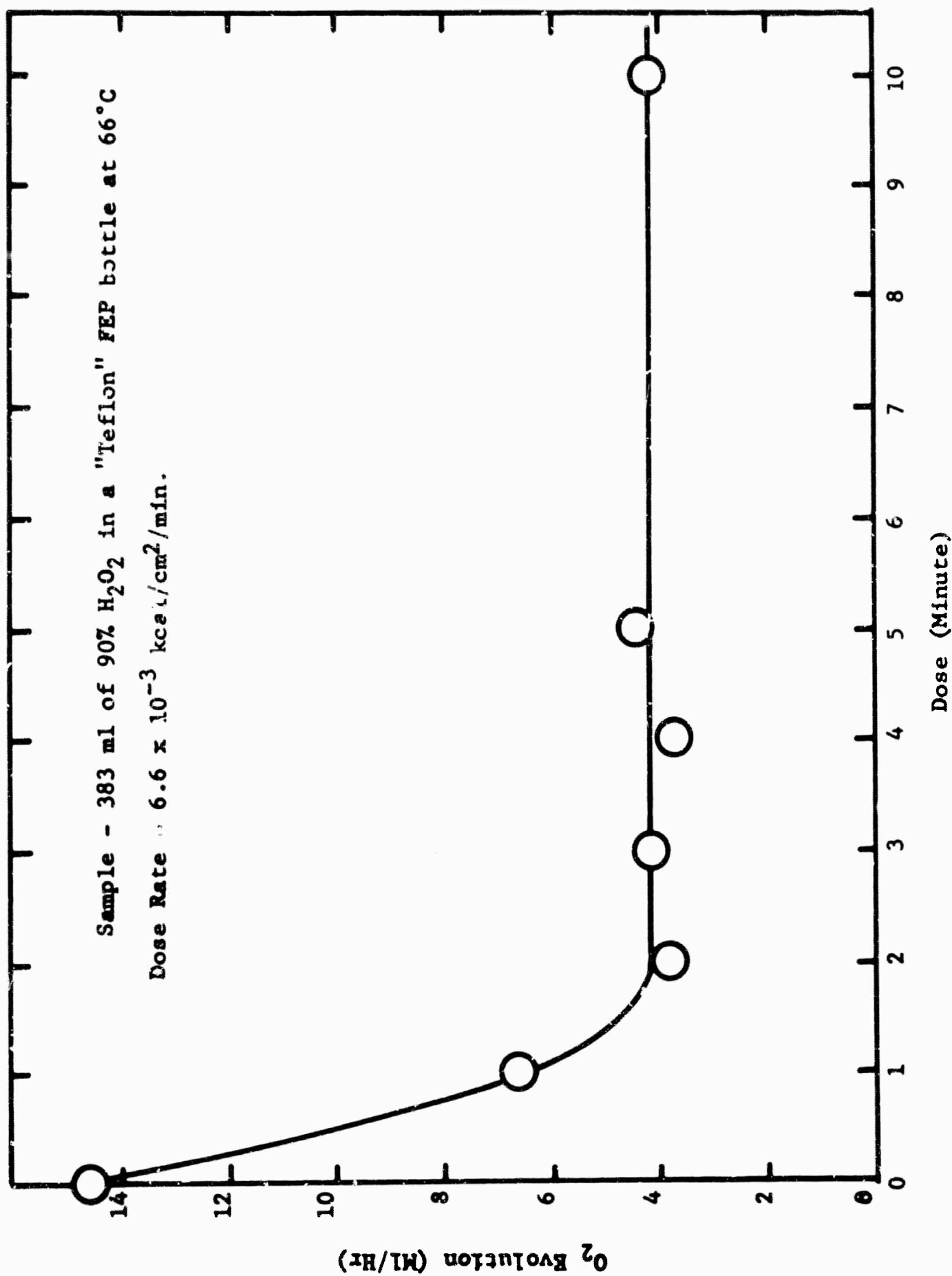
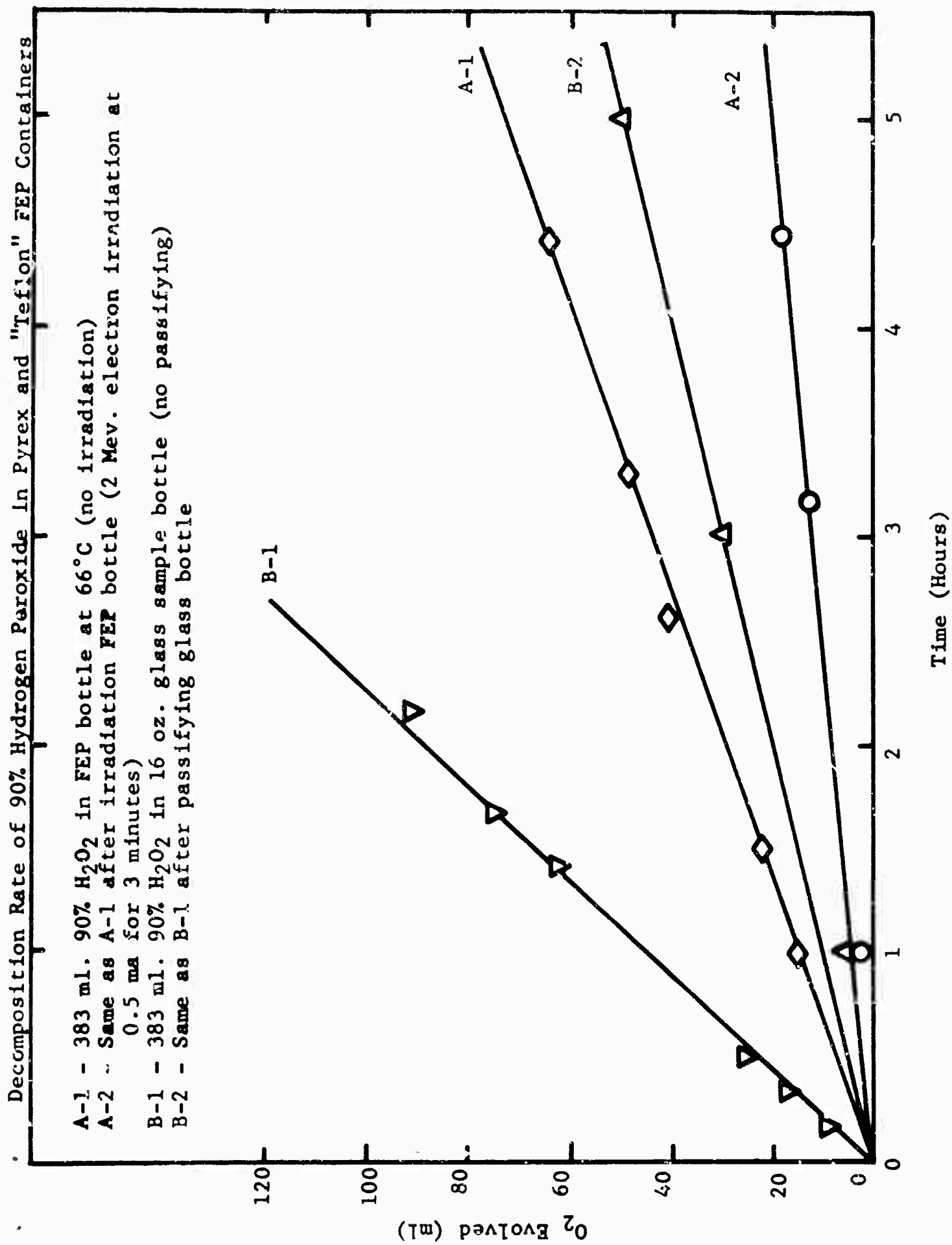


FIGURE 8



REFERENCES

1. A. M. Stock in "Stability of High Strength H_2O_2 ", Quarterly Report for period ending March 31, 1965, Contract No. AF 04(611)-10216, p. 4.
2. Anbar, M. and Thomas, J. K., J. Phys. Chem., 68, 3829 (1964).
3. Marsh, J. E., J. Chem. Soc., 1927, 3164.
4. Jurd, L., Australian J. Sci. Res., 2A, 595 (1949).
5. Johnson, B., J. Am. Chem. Soc., 65, 1218 (1943).
6. Czapski, G. and Dorfman, L.M., J. Phys. Chem., 68, 1169 (1964).
7. Saito, E. and Bielski, B. H. J., J. Am. Chem. Soc., 83, 4467 (1961).
8. Bielski, B. H. J. and Saito, E., J. Phys. Chem., 66, 2266 (1962).
9. Piette, L. H., Bulow, G. and Loeffler, K., Paper presented at the American Chemical Society Meeting, Philadelphia, Pennsylvania, April 5-10, 1964.
10. Smith, G. F., "Cerate Oxidimetry", G. F. Smith Chemical Co., Columbus, Ohio (1942).
11. Lovejoy, E. R., Bro, M. I. and Bowers, G. J., J. Applied Polymer Science 9, 401 (1965).
12. Burton, M. and Kurien, K. C., J. Phys. Chem., 63, 899 (1959).
13. Ferradini, C. and Koulkes-Pujo, A. M., J. Chim. Phys., 1310 (1963).
14. Hummel, A. and Allen, A.O., Radiation Res., 17, 302 (1962).
15. Hummel, A. and Allen, A.O., unpublished; see M. Anbar and P. Nata, International J. App. Radiation and Isotopes, 16, 227 (1965).
16. Adams, G. E. and Boag, J. W., Proc. Chem. Soc., London, 1964, 112.
17. Dainton, F. S. and Sills, S. A. Proc. Chem. Soc., London, 1962, 223.
18. Anbar, M. and Meyerstein, D., Israel AEC Semi-annual Report, IA-920, p. 108 (1964).
19. Dainton, F. S. and Hardwick, T. J., Trans. Faraday Soc., 53, 333 (1957).
20. Keene, J. P., Radiation Res., 22, 14 (1964).
21. Rothschild, W. G. and Allen, A. O., Radiation Res., 8, 101 (1958).

22. Schwarz, H. A., J. Phys. Chem., 66, 255 (1962).
23. Bum, D., Dainton, F. S., Salmon, G. A., and Hardwick, T.J., Trans. Faraday Soc., 55, 1760 (1959).
24. Rabani, J. and Stein, G., Trans. Faraday Soc., 58, 2150 (1962).
25. Boyle, J.W., Weiner, S. and Hochanadel, C. J., J. Phys. Chem., 63, 892 (1959).
26. Sworski, T. J., Radiation Res., 4, 483 (1956).
27. Sworski, T. J., Radiation Res., 6, 645 (1957).
28. Dainton, F. S. and Sills, S. A., Proc. Chem. Soc., London, 1962, 223.
29. Czapski, G., Rabani, J. and Stein, G., Trans. Faraday Soc., 58, 2160 (1962).
30. Schwarz, H. A. and Allen, A. O., J. Am. Chem. Soc., 77, 1324 (1955).